Nuclear Physics B350 (1991) 474–511
North-Holland

$U(1)_L \otimes U(1)_R$ SYMMETRIC YUKAWA MODEL IN THE SYMMETRIC PHASE

K. FARAKOS and G. KOUTSOUMBAS

National Technical University of Athens, 157 73 Zografou Campus, Athens, Greece

L. LIN, J. P. MA and I. MONTVAY

Deutsches Elektronen-Synchrotron DESY, Notkestr. 85, W-2000 Hamburg 52, Germany

G. MÜNSTER

II. Institut für Theoretische Physik der Universität Hamburg, Luruper Chaussee 149, W-2000 Hamburg 50, Germany

Received 2 May 1990
(Revised 6 August 1990)

The lattice regularized $U(1)_L \otimes U(1)_R$ symmetric scalar fermion model with explicit mirror fermions is investigated in the phase with unbroken symmetry. As a first part of a non-perturbative investigation, in the present work numerical Monte Carlo calculations with dynamical fermions are performed on $4^3 \times 8$, $6^3 \times 12$ and $8^3 \times 16$ lattices near the expected perturbative gaussian fixed point, in order to study the cutoff-dependent upper limit on the renormalized scalar quartic- and Yukawa-couplings. The bare Yukawa coupling of the mirror fermion is fixed at zero, which is near the region of parameter space where in the broken phase decoupling of the mirror fermion is expected. Lattice perturbation theory and fermion hopping parameter expansion is exploited for supporting the numerical simulations.

1. Introduction

An important part of the Standard Model of elementary particle interactions is the Higgs–Yukawa sector, where the masses of elementary particles arise due to spontaneous symmetry breaking. The couplings in this sector, namely the quartic self-coupling of the scalar field and the Yukawa couplings between the scalar field and the fermions, are not asymptotically free. On the contrary, the perturbative renormalization of these couplings is governed by an infrared fixed point at zero. In other words, these couplings are "*infrared free*", which means that if the cutoff in the field theory describing the Higgs–Yukawa sector is much larger than the physical (electroweak) scale, then the renormalized couplings are small. In fact, in

the limit of infinite cutoff the infrared free couplings have to be exactly zero: the continuum limit of such quantum field theories is "*trivial*". The perturbation theory describing the small physical Higgs- and Yukawa-couplings is defined around this "*trivial gaussian fixed point*".

Small renormalized couplings correspond to small scalar and fermion masses compared to the scalar vacuum expectation value. At present it seems probable that the two missing particles in the Standard Model, namely the top quark and the Higgs boson, are relatively heavy. Therefore, the question naturally arises how far can this perturbative picture be stretched, how large the masses produced by spontaneous symmetry breaking can be, before the perturbative description becomes inconsistent. This question obviously requires a non-perturbative framework like lattice regularization. An outcome of the non-perturbative investigations is the cutoff-dependent upper limit for the masses. In principle one can imagine two extreme situations: the upper limits can either be very large or very small. In the first case even with a very high cutoff the renormalized couplings can be strong, therefore there can in principle exist a strongly interacting Higgs–Yukawa sector which is outside of the reach of perturbation theory. In the second case, once the cutoff is a little bit higher than the physical scale, the renormalized couplings become small and there is no physical situation with strong interactions. In this case perturbation theory is always applicable. Recently substantial effort has been invested into non-perturbative lattice investigations in the pure scalar sector, neglecting Yukawa couplings, which showed that in this case the second alternative is realized (for references on this subject see ref. [1]). It is an interesting question whether the influence of strong Yukawa couplings can change the situation. This motivates a growing number of studies of Yukawa models on the lattice (see e.g. refs. [2–7] and for further references the review [8]).

In the present paper we investigate the cutoff-dependent upper limit on the renormalized couplings in the neighbourhood of the gaussian fixed point in the symmetric phase of a $U(1)_L \otimes U(1)_R$ symmetric Yukawa model with explicit mirror fermions (generally, we shall denote the fermion by ψ and its mirror fermion partner by χ). This is a first part of similar non-perturbative investigations of lattice Yukawa models. In a subsequent paper [9] we shall extend this study to the phase with broken symmetry. In the symmetric phase the mirror symmetry is unbroken, that is the fermions occur in pairs with opposite chirality. The fermion spectrum is "vectorlike", the dependence on chirality is manifested only in the Yukawa interactions. In the phase with broken symmetry the non-zero vacuum expectation value of the scalar field breaks also the mirror symmetry. The physical fermions are in general mixtures of the mirror pair with different masses [10]. In the broken phase it seems plausible that the mirror partners can be decoupled from the physical spectrum. One possible way is to introduce a second scalar field with vacuum expectation value of the order of one in lattice units and tune the Yukawa couplings in such a way that the mass of the mirror fermion also remains

of the order one (hence very large in physical units). Another, quite opposite, way proposed by Borrelli et al. [11] is to make the mirror partner massless and tune the mixing with the physical fermion to zero. This second way has the advantage that it does not require more fields and parameters.

The non-perturbative study of the symmetric phase can reveal important properties of our model. In particular, the renormalization group behaviour of the Yukawa coupling can be investigated. It is expected on general grounds, and it was also shown by non-perturbative studies in pure ϕ^4-models [12], that the qualitative features of renormalization are the same in the symmetric and broken phases. From a technical point of view the investigation of the symmetric phase is easier. First of all, the infrared singularities due to the presence of zero-mass Goldstone bosons in the broken phase require special care. A second difficulty in the broken phase is that, unlike in the symmetric phase, the fermion and boson masses cannot be tuned separately (the fermion–boson mass ratio is given by the renormalized Yukawa- and quartic-couplings). This leads in some parts of the parameter space to large mass ratios, making numerical investigations difficult. The decoupling of the fermion doublers (there are 30 of them in our formulation) can also be studied in the symmetric phase. However, as we discussed above, the fermion and mirror fermion are degenerate here, therefore the decoupling of the mirror fermion can only be investigated in the broken phase.

In the Standard Model the Higgs–Yukawa sector is coupled to the rest by the gauge couplings. Since at the electroweak scale the gauge couplings are weak, in a first approximation one can neglect them. This we do in the present paper. Nevertheless, one has to keep in mind that from the point of view of the decoupling of mirror fermion partners the electroweak chiral $SU(2)_L \otimes U(1)_Y$ gauge interaction is a non-trivial difficulty (see e.g. ref. [13]). Another simplification in the present paper is that we only consider a $U(1)_L \otimes U(1)_R$ symmetry. This has many important qualitative features in common with the $SU(2)_L \otimes SU(2)_R$ model [10] and with the $SU(2)_L \otimes U(1)_Y$ symmetric model for mirror pairs of standard fermion families [14]. In particular, due to the breaking of a continuous global symmetry in the broken phase, there is a massless Goldstone boson. From the point of view of axial anomalies this model is particularly interesting, because a U(1) axial symmetry can be anomalous [unlike SU(2)]. As far as numerical simulations are concerned, the smaller number of degrees of freedom saves computer time.

The trivial gaussian fixed point is at vanishing couplings: $\lambda = G_\psi = G_\chi = 0$ (λ is the bare scalar self-coupling, G_ψ and G_χ are the bare Yukawa couplings, and the corresponding renormalized couplings will be denoted by an index R). Therefore, we start the numerical simulation at small couplings and look how far the renormalized couplings λ_R and $G_{R\psi}$ can be increased by increasing the bare couplings (λ, G_ψ), without crossing some singularity corresponding to a phase boundary in the bare parameter space. In the present paper we fix the bare

Yukawa coupling of the mirror fermion in the numerical simulations to $G_\chi = 0$. This is because finally we are interested in the broken phase with decoupled mirror fermions. One of the decoupling conditions is $G_{R\chi} = 0$ and, as we shall show in this paper, $G_{R\chi} = 0$ roughly corresponds to $G_\chi = 0$.

The outline of this paper is as follows: in sect. 2 the lattice action and the bare parameter space will be introduced, the symmetries of the model will be considered and the renormalized quantities will be defined in a form suitable for numerical calculations. Sect. 3 is devoted to perturbation theory: the Callan–Symanzik β-functions and the finite-volume effects will be calculated on the lattice and in continuum. The unitarity condition for tree amplitudes will also be derived. In sect. 4 the fermion propagator will be considered in 7th order fermion hopping parameter expansion. The results of the numerical simulations will be presented in sect. 5. Sect. 6 contains a short summary and some concluding remarks.

2. Actions and renormalization

2.1. LATTICE ACTIONS AND PARAMETERS

The $U(1)_L \otimes U(1)_R$ symmetric model is the simplest in a general class of Yukawa models with mirror fermion pairs. The lattice action is analogous to the $SU(2)_L \otimes SU(2)_R$ symmetric one [10], and has already been defined in a previous work on the limit of infinitely heavy (static) fermions [15]. We use here the same notations as in ref. [15], that is the lattice action with a general field normalization is

$$
\begin{aligned}
S \equiv S_\phi + S_{\psi\chi\phi} = \sum_x \Big\{ & \mu_\phi \phi_x^+ \phi_x + \lambda (\phi_x^+ \phi_x)^2 - \kappa \sum_\mu \phi_{x+\hat{\mu}}^+ \phi_x \\
& + \mu_{\psi\chi} \left[(\bar{\chi}_x \psi_x) + (\bar{\psi}_x \chi_x) \right] - \sum_\mu \left[K_\psi (\bar{\psi}_{x+\hat{\mu}} \gamma_\mu \psi_x) + K_\chi (\bar{\chi}_{x+\hat{\mu}} \gamma_\mu \chi_x) \right] \\
& + K_r \sum_\mu \left[(\bar{\chi}_x \psi_x) - (\bar{\chi}_{x+\hat{\mu}} \psi_x) + (\bar{\psi}_x \chi_x) - (\bar{\psi}_{x+\hat{\mu}} \chi_x) \right] \\
& + G_\psi (\bar{\psi}_x [\phi_{1x} - i\gamma_5 \phi_{2x}] \psi_x) + G_\chi (\bar{\chi}_x [\phi_{1x} + i\gamma_5 \phi_{2x}] \chi_x) \Big\} . \qquad (1)
\end{aligned}
$$

Here x is a lattice point and the sum Σ_μ runs over eight directions of the neighbours, $\hat{\mu}$ is the unit vector in the direction of μ. The fields for the mirror fermion pair are ψ_x and χ_x, the complex scalar field is $\phi_x \equiv \phi_{1x} + i\phi_{2x}$. A

normalization convenient for the numerical simulations is defined by

$$\mu_\phi = 1 - 2\lambda\,, \qquad K_\psi = K_\chi \equiv K\,, \qquad K_r \equiv rK\,, \qquad \bar{\mu} \equiv \mu_{\psi\chi} + 8rK = 1\,. \quad (2)$$

In the present section this normalization will generally be used. However, sometimes the last condition will not be used and $\bar{\mu}$ or $\mu_{\psi\chi}$ will be explicitly written out. For the perturbative calculations other normalizations are better (see sect. 3).

The term proportional to $\mu_{\psi\chi}$ in the action is a chiral invariant mass term for the fermions. The term proportional to K_r is a chiral invariant Wilson term which serves to give the fermion doublers masses of the order of the cutoff as explained below.

The fermionic part of the action $S_{\psi\chi\phi}$ can be written with the help of the "*fermion matrix*" $Q(\phi)_{yx}$ as

$$S_{\psi\chi\phi} = \sum_{x,y} \bar{\Psi}_y Q(\phi)_{yx} \Psi_x\,. \quad (3)$$

Here the fermion field $\Psi_x \equiv (\psi_x, \chi_x)$ stands for the mirror pair, and the $8 \otimes 8$ matrix Q is given in a $2 \otimes 2$ block notation by

$$Q(\phi)_{yx} = \delta_{yx} \begin{pmatrix} G_\psi \phi_x^+ & 0 & \bar{\mu} & 0 \\ 0 & G_\psi \phi_x & 0 & \bar{\mu} \\ \bar{\mu} & 0 & G_\chi \phi_x & 0 \\ 0 & \bar{\mu} & 0 & G_\chi \phi_x^+ \end{pmatrix}$$

$$- K \sum_\mu \delta_{y,x+\hat{\mu}} \begin{pmatrix} 0 & \Sigma_\mu & r & 0 \\ \bar{\Sigma}_\mu & 0 & 0 & r \\ r & 0 & 0 & \Sigma_\mu \\ 0 & r & \bar{\Sigma}_\mu & 0 \end{pmatrix}. \quad (4)$$

This is on a chiral basis, that is the euclidean γ-matrices are defined as

$$\gamma_\mu = \begin{pmatrix} 0 & \Sigma_\mu \\ \bar{\Sigma}_\mu & 0 \end{pmatrix}, \qquad \gamma_5 = \begin{pmatrix} 1 & 0 \\ 0 & -1 \end{pmatrix}. \quad (5)$$

Here, for $\mu = 1,2,3$, $\Sigma_\mu = -\bar{\Sigma}_\mu = -i\sigma_\mu$ and $\Sigma_4 = \bar{\Sigma}_4 = 1$ ($\sigma_{1,2,3}$ denote the Pauli matrices). For negative indices the definition is given by $\Sigma_\mu \equiv -\Sigma_{-\mu}$.

In the numerical simulations we shall use the Hybrid Monte Carlo algorithm for dynamical fermions [16]. This requires a flavour doubling of the fermion spectrum:

the fermion part of the lattice action will be, instead of eq. (3),

$$S_{\psi\chi\phi} = \sum_{f=1,2} \sum_{x,y} \bar{\Psi}_y^{(f)} Q(\phi)_{yx}^{(f)} \Psi_x^{(f)}. \tag{6}$$

For the value $f = 1$ of the flavour index the fermion matrix is the same as before: $Q^{(1)} = Q$, but for the other value $f = 2$ the adjoint is taken: $Q^{(2)} = Q^+$. This means that the ψ-field of the second flavour is a mirror fermion with respect to the ψ-field of the first one. (Note, however, that these fields transform differently under the exactly conserved vectorlike $U(1)_{1-2}$ defined below.) Let us emphasize that this flavour doubling is of purely technical origin. It has nothing to do with the mirror doubling problem on the lattice [17]. The original model with the action (1) can be studied non-perturbatively, for instance, by the fermion hopping parameter expansion (see sect. 4).

The global symmetries of the flavour-doubled model can be defined by the transformations

$$\begin{aligned}
&\psi_{Lx}^{(f)\prime} = e^{-i\alpha_{fL}} \psi_{Lx}^{(f)}, \quad \psi_{Rx}^{(f)\prime} = e^{-i\alpha_{fR}} \psi_{Rx}^{(f)}, \quad \chi_{Rx}^{(f)\prime} = e^{-i\alpha_{fL}} \chi_{Rx}^{(f)}, \quad \chi_{Lx}^{(f)\prime} = e^{-i\alpha_{fR}} \chi_{Lx}^{(f)} \\
&\bar{\psi}_{Lx}^{(f)\prime} = \bar{\psi}_{Lx}^{(f)} e^{i\alpha_{fL}}, \quad \bar{\chi}_{Rx}^{(f)\prime} = \bar{\chi}_{Rx}^{(f)} e^{i\alpha_{fR}}, \quad \bar{\chi}_{Rx}^{(f)\prime} = \bar{\chi}_{Rx}^{(f)} e^{i\alpha_{fL}}, \quad \bar{\chi}_{Lx}^{(f)\prime} = \bar{\chi}_{Lx}^{(f)} e^{i\alpha_{fR}}.
\end{aligned} \tag{7}$$

Consistency for the transformation of the scalar field requires

$$\alpha_{1L} = \alpha_L + \alpha_{1-2}, \quad \alpha_{1R} = \alpha_R + \alpha_{1-2}, \quad \alpha_{2L} = \alpha_R - \alpha_{1-2}, \quad \alpha_{2R} = \alpha_L - \alpha_{1-2}. \tag{8}$$

The scalar field is then transformed as

$$\phi_x' = e^{-i(\alpha_L - \alpha_R)} \phi_x. \tag{9}$$

Eqs. (7)–(9) define a global symmetry $U(1)_L \otimes U(1)_R \otimes U(1)_{1-2}$. The last factor is a vectorlike symmetry implying the conservation of the number of fermions with first flavour minus the number of fermions with second flavour. The sum of the flavour numbers is also conserved due to $U(1)_L \otimes U(1)_R$, therefore the $U(1)_L \otimes U(1)_R \otimes U(1)_{1-2}$ symmetry implies the conservation of both flavour numbers.

After fixing the field normalizations, the $U(1)_L \otimes U(1)_R$ symmetric Yukawa model has altogether 5 independent parameters: 2 mass parameters κ and K, and 3 coupling parameters λ, G_ψ and G_χ. This relatively large number of parameters makes the numerical simulation rather demanding. In any case it is very useful to have some, at least qualitative, information about different limits. It is convenient first to fix the bare scalar quartic coupling λ. For reasons explained below, in the numerical simulations we shall also fix the bare Yukawa coupling G_χ (actually to

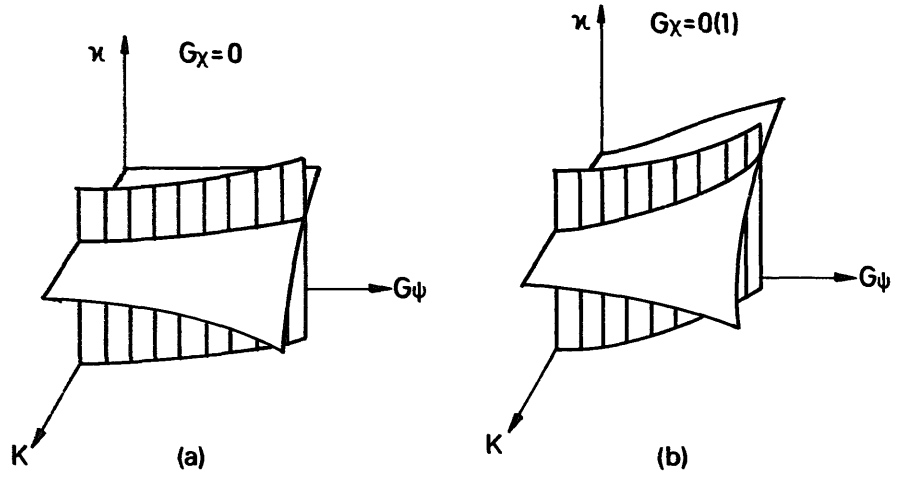

Fig. 1. (a) The qualitative phase structure in the (κ, K, G_ψ)-plane in the neighbourhood of the gaussian fixed point, for $G_\chi = 0$ and any fixed λ. The symmetric and broken phases are separated from each other by the two critical surfaces where, respectively, the scalar and fermion masses vanish. The intersection of these two surfaces is the multicritical line where both scalar and fermion masses are zero. (b) The same as (a) for $G_\chi = O(1)$ and λ = finite. The picture for infinite λ is similar, but then the phase transition line in the $K = 0$ plane is a constant as a function of G_ψ (see ref. [15]), and the critical surface for vanishing fermion mass touches the $K = 0$ plane.

the value $G_\chi = 0$). Therefore, let us consider the space of three parameters (κ, K, G_ψ) for not too large values of these variables, which are relevant for the symmetric phase in the neighbourhood of the gaussian fixed point at ($\lambda = G_\psi = G_\chi = 0$, $\kappa = rK = \frac{1}{8}$).

The expected phase structure for zero and O(1) values of G_χ is shown, respectively, in fig. 1a and fig. 1b. The plane $G_\psi = 0$ in fig. 1a is the trivial limit of uncoupled free fermion fields. Due to the symmetry with respect to the exchange of ψ and χ, the $G_\psi = 0$ plane in fig. 1b is equivalent to a part of fig. 1a. The limit of static fermions at $K = 0$ was investigated in detail by three of us in a previous publication [15], using scalar hopping parameter expansion and numerical simulations. In this limit the fermion determinant is local and can explicitly be taken into account. In the effective scalar model at $K = 0$ there are two phases: a symmetric phase at small κ and a broken phase at larger κ. The phase transition between these two phases is of second order for small and large values of the product $G_\psi G_\chi$. At intermediate values of $G_\psi G_\chi$ and $\lambda \neq \infty$, the phase transition is of first order and is accompanied by a jump in the average field length. In the limit $\lambda \to \infty$, the first-order phase transition line disappears by shrinking to the point $G_\psi G_\chi = 1$. For finite λ the phase transition line in the $K = 0$ plane depends on G_ψ, but at $\lambda = \infty$ it is a constant. In the plane $\kappa = 0$ non-perturbative information can be obtained from an expansion in powers of the fermion hopping parameter K. In the $SU(2)_L \otimes SU(2)_R$ model this has recently been done in refs. [18, 19]. The qualitative behaviour in the $U(1)_L \otimes U(1)_R$ model is similar (see sect. 4). At $\lambda = \infty$, where

up to now most of the fermion hopping parameter expansions were done, the critical line for vanishing fermion masses touches the $K=0$ plane at $G_\psi G_\chi = 1$.

The phase transitions at the boundaries $K=0$ and $\kappa=0$ are continued inside the (κ, K, G_ψ)-space (see figs. 1a,b). The critical line in the $K=0$ plane is continued as a critical surface, where the scalar mass is zero. As a continuation of the critical line in the $\kappa=0$ plane, there is another critical surface where the fermion mass vanishes. The intersection of these two surfaces is the "multicritical line", where both scalar and fermion masses vanish. Continuum limits can be defined by going to some of the points of this multicritical line. The two critical surfaces separate the symmetric phase and the broken phase. The symmetric phases is in the corner at small κ and K. The rest is the broken phase.

An interesting feature is that for $\lambda = \infty$ the critical surface for the fermion mass touches the $K=0$ plane at $G_\psi G_\chi = 1$. This comes out of the fermion hopping parameter expansion, as it was first observed in ref. [18]. In fact, in ref. [18] the critical line for the fermion mass was continued to negative values. However, in the normalization convention $\bar{\mu}=1$ the transformation $K \to -K$ can be compensated in the lattice action by a "staggered" transformation of the fermion field

$$\Psi_x \to (-1)^{x_1+x_2+x_3+x_4}\Psi_x, \qquad \bar{\Psi}_x \to (-1)^{x_1+x_2+x_3+x_4}\bar{\Psi}_x \tag{10}$$

($x_{1,2,3,4}$ are the lattice coordinates to the point x). Because of

$$(-1)^{x_1+x_2+x_3+x_4} = e^{\pm i\pi(x_1+x_2+x_3+x_4)}, \tag{11}$$

after Fourier transforming to momentum space the transformation in eq. (10) means a shift in all momentum components by $\pm\pi$, that is going to the opposite corner of the Brillouin zone.

On a finite lattice we assume periodic or antiperiodic boundary conditions for the fields. Specifically, the scalar field is periodic in all directions, the fermion field is periodic in space directions and antiperiodic in the time direction. Therefore, on a $L^3 \times T$ lattice the allowed values of momentum components are

$$p_i = \frac{2\pi}{L} n_i, \quad n_i = 0,1,2,\ldots,L-1, \qquad i=1,2,3,$$

$$p_4 = \frac{2\pi}{T}(n_4+\delta_4), \quad n_4 = 0,1,2,\ldots,T-1. \tag{12}$$

Here, for bosons $\delta_4 = 0$ and for fermions $\delta_4 = \frac{1}{2}$.

The reason for introducing in the lattice action (1) the chiral invariant Wilson term proportional to the parameter r is to remove the fermion doublers from the physical spectrum. In the case of free fermions the fermion spectrum can be

inferred from the free fermion propagator which, for a general field normalization, is

$$\Delta^{\Psi}_{yx} = \frac{1}{L^3 T} \sum_p e^{ip\cdot(y-x)} \left[4K^2 \bar{p}^2 + \left(\mu_{\psi\chi} + rK\hat{p}^2 \right)^2 \right]^{-1} \begin{pmatrix} -2Ki\gamma\cdot\bar{p} & \mu_{\psi\chi} + rK\hat{p}^2 \\ \mu_{\psi\chi} + rK\hat{p}^2 & -2Ki\gamma\cdot\bar{p} \end{pmatrix}. \tag{13}$$

Here the notations $\bar{p}_\mu \equiv \sin p_\mu$ and $\hat{p}_\mu \equiv 2\sin(\frac{1}{2}p_\mu)$ are used. This shows that in the continuum limit, when $p_\mu \to 0$ ($\mu = 1,2,3,4$), the term proportional to r vanishes, but at any other corner of the Brillouin zone, where some $p_\mu = \pm\pi$, the fermion doublers get a mass which is of the order of $r = \mathrm{O}(1)$ in lattice units. The important question is, of course, whether this remains so after switching on the Yukawa interactions. A hint that at strong bare Yukawa couplings some doublers may remain in the physical spectrum was obtained in the sigma model with Wilson lattice fermions [20]. In this model at infinitely strong bare Yukawa coupling, in the random walk approximation to the hopping parameter expansion, the doubler at $p = (\pi,\pi,\pi,\pi)$ becomes degenerate to the state at $p = (0,0,0,0)$. The same happens also in the $\mathrm{SU(2)_L} \otimes \mathrm{SU(2)_R}$ symmetric Yukawa model with explicit mirror fermions for $G_\psi = G_\chi = \infty$ [18]. Therefore in non-perturbative studies it is important to observe the fermion masses at every corner of the Brillouin zone. This point will be discussed further in sect. 5.

2.2. RENORMALIZED QUANTITIES

Since in the symmetric phase both fermions and bosons are massive, the renormalization can be defined at zero four-momentum without a danger of infrared singularities. The two flavours are separately conserved, therefore in this subsection we only consider a single fermion–mirror-fermion pair $\Psi \equiv (\psi, \chi)$. The behaviour of the fermion propagator matrix in momentum space for $p \to 0$ is

$$\tilde{\Delta}_\Psi(p) \equiv \sum_x e^{-ip\cdot(y-x)} \Delta^{\Psi}_{yx} = A - ip\cdot\gamma B + \mathrm{O}(p^2). \tag{14}$$

The inverse propagator in the same limit is

$$\tilde{\Delta}_\Psi(p)^{-1} = M + ip\cdot\gamma N + \mathrm{O}(p^2), \tag{15}$$

where the matrices M and N are given by

$$M = A^{-1}, \qquad N = A^{-1} B A^{-1}. \tag{16}$$

The matrices A and B can be determined in a numerical simulation from the expectation values of fermionic time slices. Taking into account that, due to the

boundary conditions, only the discrete momentum values in eq. (12) are allowed, possible definitions on the lattice are

$$A = \frac{1}{2}\left[\tilde{\Delta}_\Psi\left(0,0,0,+\frac{\pi}{T}\right) + \tilde{\Delta}_\Psi\left(0,0,0,-\frac{\pi}{T}\right)\right]$$
$$= \sum_x \cos\left[\frac{\pi}{T}(y_4 - x_4)\right]\Delta^\Psi_{yx}$$
$$= \sum_x \cos\left[\frac{\pi}{T}(y_4 - x_4)\right]\langle \Psi_y \bar{\Psi}_x \rangle,$$
$$B\gamma_4 = \frac{i}{2\sin(\pi/T)}\left[\tilde{\Delta}_\Psi\left(0,0,0,+\frac{\pi}{T}\right) - \tilde{\Delta}_\Psi\left(0,0,0,-\frac{\pi}{T}\right)\right]$$
$$= \sum_x \frac{\sin[(\pi/T)(y_4 - x_4)]}{\sin(\pi/T)}\Delta^\Psi_{yx}$$
$$= \sum_x \frac{\sin[(\pi/T)(y_4 - x_4)]}{\sin(\pi/T)}\langle \Psi_y \bar{\Psi}_x \rangle. \tag{17}$$

Here, as usual, $\langle \ldots \rangle$ denotes an expectation value with respect to the Boltzmann factor e^{-S} and, for instance, x_4 is the time coordinate of the lattice point $x \equiv (x_1, x_2, x_3, x_4)$.

In the symmetric phase, due to chiral symmetry, the matrices A, B have in the (ψ, χ)-space the general form

$$A = \begin{pmatrix} 0 & A_{\psi\chi} \\ A_{\psi\chi} & 0 \end{pmatrix}, \qquad B = \begin{pmatrix} B_{\psi\psi} & 0 \\ 0 & B_{\chi\chi} \end{pmatrix}. \tag{18}$$

Therefore, M and N are given by

$$M = \begin{pmatrix} 0 & A^{-1}_{\psi\chi} \\ A^{-1}_{\psi\chi} & 0 \end{pmatrix}, \qquad N = \begin{pmatrix} B_{\chi\chi}A^{-2}_{\psi\chi} & 0 \\ 0 & B_{\psi\psi}A^{-2}_{\psi\chi} \end{pmatrix}. \tag{19}$$

The wave function renormalization has to transform N to the unit matrix. Let us define the renormalized fermion fields by

$$\Psi_R \equiv Z_\Psi^{-1/2}\Psi, \qquad \bar{\Psi}_R \equiv \bar{\Psi} Z_\Psi^{-1/2}. \tag{20}$$

According to eq. (19) the matrix $Z_\Psi^{1/2}$ is given by

$$Z_\Psi^{1/2} \equiv \begin{pmatrix} \sqrt{Z_\psi} & 0 \\ 0 & \sqrt{Z_\chi} \end{pmatrix} = \begin{pmatrix} A_{\psi\chi}B^{-1/2}_{\chi\chi} & 0 \\ 0 & A_{\psi\chi}B^{-1/2}_{\psi\psi} \end{pmatrix}. \tag{21}$$

Multiplying the unrenormalized mass matrix M by $Z_\psi^{1/2}$ from left and right gives the renormalized mass matrix M_R and renormalized mass μ_R,

$$M_R \equiv Z_\psi^{1/2} M Z_\psi^{1/2} = \begin{pmatrix} 0 & A_{\psi\chi}(B_{\psi\psi}B_{\chi\chi})^{-1/2} \\ A_{\psi\chi}(B_{\psi\psi}B_{\chi\chi})^{-1/2} & 0 \end{pmatrix} \equiv \begin{pmatrix} 0 & \mu_R \\ \mu_R & 0 \end{pmatrix}. \tag{22}$$

The renormalized fermion mass matrix M_R can be diagonalized by a (physical) orthogonal transformation. This corresponds to an orthogonal transformation of the renormalized fermion fields. However, as it is clear from eq. (22), one of the mass eigenvalues is negative. The negative fermion mass can be turned to a positive one by a γ_5-transformation, therefore the diagonalization to positive mass eigenvalues is as follows:

$$\bar{O}^+ M_R O = \begin{pmatrix} \mu_R & 0 \\ 0 & \mu_R \end{pmatrix}, \quad O = \frac{1}{\sqrt{2}} \begin{pmatrix} 1 & -\gamma_5 \\ 1 & \gamma_5 \end{pmatrix}, \quad \bar{O}^+ = \frac{1}{\sqrt{2}} \begin{pmatrix} 1 & 1 \\ \gamma_5 & -\gamma_5 \end{pmatrix}. \tag{23}$$

Since in the symmetric phase the masses of the fermion and mirror fermion are the same, the diagonalization of the fermion mass matrix is not unique. Another interesting way of diagonalization can be achieved by

$$\bar{U}^+ M_R U = \begin{pmatrix} \mu_R & 0 \\ 0 & \mu_R \end{pmatrix}, \quad U = \begin{pmatrix} P_L & P_R \\ P_R & P_L \end{pmatrix}, \quad \bar{U}^+ = \begin{pmatrix} P_R & P_L \\ P_L & P_R \end{pmatrix}. \tag{24}$$

Here $P_{L,R}$ are chiral projectors: $P_L = \frac{1}{2}(1+\gamma_5)$, $P_R = \frac{1}{2}(1-\gamma_5)$. This way of diagonalization means that the left- and right-handed components of ψ and χ are reshuffled in order to obtain a vector-like kinetic part. Sometimes it is advantageous to do this directly in the action, especially for applications in the symmetric phase (see, for instance, the hopping parameter expansion in sect. 4).

The new fields are

$$\psi_{Ax} \equiv \psi_{Lx} + \chi_{Rx}, \quad \psi_{Bx} \equiv \chi_{Lx} + \psi_{Rx}, \quad \bar{\psi}_{Ax} \equiv \bar{\psi}_{Lx} + \bar{\chi}_{Rx}, \quad \bar{\psi}_{Bx} \equiv \bar{\chi}_{Lx} + \bar{\psi}_{Rx}. \tag{25}$$

Denoting now the (ψ_A, ψ_B)-pair by $\Psi_x \equiv (\psi_{Ax}, \psi_{Bx})$, and using the field normaliza-

tion condition in eq. (2), $\bar{\mu} = 1$, the fermion matrix in eq. (3) becomes

$$\bar{Q}(\phi)_{yx} = \begin{pmatrix} \delta_{yx} - K\Sigma_\mu \delta_{y,x+\hat{\mu}}(\gamma_\mu + r) & \delta_{yx}\phi_x(G_\alpha - \gamma_5 G_\beta) \\ \delta_{yx}\phi_x^+(G_\alpha + \gamma_5 G_\beta) & \delta_{yx} - K\Sigma_\mu \delta_{y,x+\hat{\mu}}(\gamma_\mu + r) \end{pmatrix}. \quad (26)$$

In contrast to eq. (4), this is in $4 \otimes 4$ block notation (in the (ψ_A, ψ_B)-space). The coupling constant combinations $G_{\alpha,\beta}$ are defined as

$$G_\alpha \equiv \tfrac{1}{2}(G_\psi + G_\chi), \qquad G_\beta \equiv \tfrac{1}{2}(G_\psi - G_\chi). \quad (27)$$

The result of the transformation (25) is that the fermion action without interaction becomes diagonal in ψ_A, ψ_B and equals the free Wilson action [21].

The main interest in Yukawa models with explicit mirror fermions is, however, in the phase with broken symmetry, where the two fermion masses are generally different. Therefore, the only possible way of fermion mass diagonalization there is a generalization of eq. (23). For instance, the decoupling of the mirror fermion χ can be formulated as a special case of this sort of diagonalization (see in ref. [9]).

In order to define the renormalized Yukawa couplings in terms of the expectation values on the lattice, let us introduce some shorthand notations. For instance, the type of bilinear fermionic expectation values occurring in eq. (17) can be denoted as

$$\langle \psi_L \bar{\chi}_R \rangle_0 \delta_{\rho\sigma} \equiv \frac{1}{L^3 T} \sum_{x,y} e^{-i(\pi/T)(y_4 - x_4)} \langle \psi_{yL\rho} \bar{\chi}_{xR\sigma} \rangle. \quad (28)$$

Here ρ, σ are the spinor indices of the chiral components of fermion fields. Similarly, the fermion–fermion–scalar expectation values for the renormalized Yukawa couplings are introduced as, for instance

$$\langle \psi_L \phi^+ \bar{\psi}_R \rangle_0 \delta_{\rho\sigma} \equiv \frac{1}{L^3 T} \sum_{x,y,z} e^{-i(\pi/T)(y_4 - x_4)} \langle \psi_{yL\rho} \phi_z^+ \bar{\psi}_{xR\sigma} \rangle. \quad (29)$$

The diagonal matrix built from these expectation values is

$$\langle \Psi \Phi \bar{\Psi} \rangle_0 \equiv \mathrm{diag}\{\langle \psi_L \phi^+ \bar{\psi}_R \rangle_0, \langle \psi_R \phi \bar{\psi}_L \rangle_0, \langle \chi_L \phi \bar{\chi}_R \rangle_0, \langle \chi_R \phi^+ \bar{\chi}_L \rangle_0\}. \quad (30)$$

Using these notations the renormalized Yukawa coupling matrix in the space of chiral components $(\psi_L, \psi_R, \chi_L, \chi_R)$ is defined as

$$G_R \equiv -\frac{m_R^2}{\sqrt{2Z_\phi}} M_R Z_\Psi^{-1/2} \langle \Psi \Phi \bar{\Psi} \rangle_0 Z_\Psi^{-1/2} M_R. \quad (31)$$

This is given directly in terms of the expectation values, but one can easily see that it is equivalent to the usual definition in terms of the vertex functions (see sect. 3). G_R is a diagonal matrix, $G_R = \mathrm{diag}\{G_{R\psi}, G_{R\psi}, G_{R\chi}, G_{R\chi}\}$, where

$$G_{R\psi} = -\frac{m_R^2 \mu_R^2}{Z_\chi \sqrt{2Z_\phi}} \langle \chi_L \phi \bar{\chi}_R \rangle_0 = -\frac{m_R^2 \mu_R^2}{Z_\chi \sqrt{2Z_\phi}} \langle \chi_R \phi^+ \bar{\chi}_L \rangle_0$$

$$G_{R\chi} = -\frac{m_R^2 \mu_R^2}{Z_\psi \sqrt{2Z_\phi}} \langle \psi_L \phi^+ \bar{\psi}_R \rangle_0 = -\frac{m_R^2 \mu_R^2}{Z_\psi \sqrt{2Z_\phi}} \langle \psi_R \phi \bar{\psi}_L \rangle_0 . \tag{32}$$

Here m_R is the renormalized boson mass and Z_ϕ is the wave function renormalization factor of the scalar field (The renormalized quantities in the pure ϕ^4 scalar sector are defined in the same way as in ref. [12]. See also sect. 3.) Equivalent expressions useful for the numerical determination are

$$G_{R\psi} = -\frac{Z_\psi \sqrt{2Z_\phi} \langle \chi_L \phi \bar{\chi}_R \rangle_0}{\langle \phi^+ \phi \rangle_0 \langle \chi_L \bar{\psi}_R \rangle_0 \langle \psi_L \bar{\chi}_R \rangle_0} = -\frac{Z_\psi \sqrt{2Z_\phi} \langle \chi_R \phi^+ \bar{\chi}_L \rangle_0}{\langle \phi^+ \phi \rangle_0 \langle \chi_R \bar{\psi}_L \rangle_0 \langle \psi_R \bar{\chi}_L \rangle_0}$$

$$G_{R\chi} = -\frac{Z_\chi \sqrt{2Z_\phi} \langle \psi_L \phi^+ \bar{\psi}_R \rangle_0}{\langle \phi^+ \phi \rangle_0 \langle \psi_L \bar{\chi}_R \rangle_0 \langle \chi_L \bar{\psi}_R \rangle_0} = -\frac{Z_\chi \sqrt{2Z_\phi} \langle \psi_R \phi \bar{\psi}_L \rangle_0}{\langle \phi^+ \phi \rangle_0 \langle \psi_R \bar{\chi}_L \rangle_0 \langle \chi_R \bar{\psi}_L \rangle_0} . \tag{33}$$

Particularly simple combinations are

$$G_{R\psi} G_{R\chi} = \frac{m_R^2 \mu_R^2 \langle \psi_L \phi^+ \bar{\psi}_R \rangle_0 \langle \chi_L \phi \bar{\chi}_R \rangle_0}{\langle \phi^+ \phi \rangle_0 \langle \psi_L \bar{\chi}_R \rangle_0 \langle \chi_L \bar{\psi}_R \rangle_0} = \frac{m_R^2 \mu_R^2 \langle \psi_R \phi \bar{\psi}_L \rangle_0 \langle \chi_R \phi^+ \bar{\chi}_L \rangle_0}{\langle \phi^+ \phi \rangle_0 \langle \psi_R \bar{\chi}_L \rangle_0 \langle \chi_R \bar{\psi}_L \rangle_0} . \tag{34}$$

In eqs. (33) and (34) the zero-momentum scalar expectation value is defined as

$$\langle \phi^+ \phi \rangle_0 \equiv \frac{1}{L^3 T} \sum_{x,y} \langle \phi_y^+ \phi_x \rangle = \frac{2Z_\phi}{m_R^2} . \tag{35}$$

Very similar expressions for the fermionic renormalized quantities can also be defined at the other corners of the Brillouin zone. The only change is that in the definitions like in eqs. (28) and (29) one has to go to the other corners of the Brillouin zone by a transformation similar to (10), (11).

3. Lattice perturbation theory

3.1. GENERAL CONSIDERATIONS

In the domain of the trivial fixed point ordinary perturbation theory can be applied to study the Yukawa model. This amounts to an expansion in the scalar

self-coupling λ and in the Yukawa couplings G_ψ and G_χ around zero. For this purpose it is convenient to rescale the fields and the couplings in such a way that the form of the action corresponds to the continuum conventions. The bare scalar field ϕ_0 and its components ϕ_{0k} are defined through

$$\sqrt{\kappa}\,\phi = \phi_0 = \frac{1}{\sqrt{2}}(\phi_{01} + i\phi_{02})\,. \tag{36}$$

The lattice lagrangian for the scalar field then reads

$$\mathscr{L}_\phi = (\partial_\mu \phi_0)^+ \partial^\mu \phi_0 + m_0^2 \phi_0^+ \phi_0 + \tfrac{1}{6} g_0 (\phi_0^+ \phi_0)^2, \tag{37}$$

where ∂_μ denotes a lattice derivative (i.e. finite difference) and the bare mass m_0 and bare coupling g_0 are given by

$$m_0^2 = \frac{\mu_\phi}{\kappa} - 8, \qquad g_0 = \frac{6\lambda}{\kappa^2}\,. \tag{38}$$

Similarly, the bare fermion and mirror fermion fields are defined by

$$\psi_0 = \sqrt{2K}\,\psi, \qquad \chi_0 = \sqrt{2K}\,\chi, \tag{39}$$

and the free part of the fermion lagrangian for one flavour is

$$\mathscr{L}_\psi = -\sum_{\mu=1}^{4} \Big\{ \tfrac{1}{2}\big(\bar\psi_{0,x+\hat\mu} - \bar\psi_{0,x-\hat\mu}\big)\gamma_\mu \psi_{0,x} + \tfrac{1}{2} r\big(\bar\chi_{0,x+\hat\mu} + \bar\chi_{0,x-\hat\mu} - 2\bar\chi_{0,x}\big)\psi_{0,x} + (\psi \leftrightarrow \chi)\Big\} + \mu_0\big(\bar\chi_{0,x}\psi_{0,x} + \bar\psi_{0,x}\chi_{0,x}\big), \tag{40}$$

with

$$\mu_0 = \mu_{\psi\chi}/2K\,. \tag{41}$$

For simplicity of the notation we display the conventions for one fermion flavour only. The perturbative results below, however, refer to the full model with two flavours of fermions and mirror fermions. Introducing the two-component vector

$$\Psi_0 = \begin{pmatrix} \psi_0 \\ \chi_0 \end{pmatrix}, \tag{42}$$

the free fermion action can be written as

$$S_\Psi = \sum_{xy} \bar\Psi_{0,y} W_{yx} \Psi_{0,x}\,, \tag{43}$$

with W_{yx} being a 2×2 matrix in (ψ, χ)-space. The Yukawa interaction is

$$S_Y = \sum_x \bar{\Psi}_{0,x} V_i \phi_{0i} \Psi_{0,x}, \tag{44}$$

where the coupling matrices V_i are

$$V_i = \begin{pmatrix} G_{0\psi} \Gamma_i & 0 \\ 0 & G_{0\chi} \Gamma_i^+ \end{pmatrix}, \tag{45}$$

with

$$G_{0\psi} = \frac{G_\psi}{2K\sqrt{2\kappa}}, \qquad G_{0\chi} = \frac{G_\chi}{2K\sqrt{2\kappa}}, \tag{46}$$

$$\Gamma_1 = 1, \qquad \Gamma_2 = -i\gamma_5. \tag{47}$$

From the expressions above the Feynman rules are derived in the usual way. We shall present them in momentum space. On a finite $L^3 \times T$ lattice the allowed momenta are in the Brillouin zone, eq. (12). For later convenience we introduce the following abbreviations:

$$\hat{p}_\mu = 2\sin\left(\frac{p_\mu}{2}\right), \qquad \bar{p}_\mu = \sin(p_\mu), \qquad \bar{\bar{p}}_\mu = \tfrac{1}{2}\sin(2p_\mu). \tag{48}$$

The scalar propagator is

$$\tilde{\Delta}_{ij}(p) = \delta_{ij} \tilde{\Delta}(p), \qquad \tilde{\Delta}(p) = \left(\hat{p}^2 + m_0^2\right)^{-1}, \tag{49}$$

and the scalar four-point vertex is

$$-g_0 S_{ijkl}, \qquad i,j,k,l = 1,2, \tag{50}$$

with

$$S_{ijkl} = \tfrac{1}{3}\left(\delta_{ij}\delta_{kl} + \delta_{ik}\delta_{jl} + \delta_{il}\delta_{jk}\right). \tag{51}$$

The kinetic term for the fermion reads in momentum space

$$\tilde{W}(p) = \sum_x e^{-ip\cdot(y-x)} W_{yx} = \begin{pmatrix} i\gamma\cdot\bar{p} & \mu_p \\ \mu_p & i\gamma\cdot\bar{p} \end{pmatrix}, \tag{52}$$

where

$$\mu_p = \mu_0 + \tfrac{1}{2} r \hat{p}^2. \tag{53}$$

Its inverse yields the fermion propagator

$$\tilde{W}(p)^{-1} = \left(\bar{p}^2 + \mu_p^2\right)^{-1} \begin{pmatrix} -i\gamma\cdot\bar{p} & \mu_p \\ \mu_p & -i\gamma\cdot\bar{p} \end{pmatrix}. \tag{54}$$

If $r > 0$ there are no doubler poles at $p_\mu = \pm\pi$. Finally the Yukawa interaction vertex between two fermions and the scalar field ϕ_{0i} is given by the matrix $-V_i$ defined above.

Using these propagators and vertices the Green functions and vertex functions are calculated in the usual way. Momentum sums or integrals respectively only run over the Brillouin zone specified above. They are denoted by

$$\int_p = \frac{1}{L^3 T} \sum_p = (2\pi)^{-4} \int_0^{2\pi} \mathrm{d}^4 p \qquad \text{if } L, T = \infty. \tag{55}$$

In the following we consider the vertex functions

$$\Gamma^{(n_B, 2n_F)}(p_a), \qquad a = 1, \ldots, n_B + 2n_F$$

for n_B bosons, n_F fermions and n_F anti-fermions. They refer to the fields ϕ, ψ, χ, $\bar{\psi}$ and $\bar{\chi}$ in the original normalization.

$\Gamma^{(2,0)}$ is the negative inverse propagator of the field $\phi(x)$. In the one-loop approximation perturbation theory yields

$$\Gamma_{ij}^{(2,0)}(p) = -\delta_{ij} Z_\phi^{-1} \{ m_R^2 + p^2 + O(p^4) \}, \tag{56}$$

where the wave function renormalization is given by

$$\begin{aligned} 2\kappa Z_\phi = 1 &- \int_p \frac{G_{0\psi} G_{0\chi} \mu_p r (8 - \hat{p}^2) + \left(G_{0\psi}^2 + G_{0\chi}^2\right) \bar{p}^2}{\left(\bar{p}^2 + \mu_p^2\right)^2} \\ &+ 4 \int_p \frac{2 G_{0\psi} G_{0\chi} \mu_p r \left(\bar{p}\cdot\bar{\bar{p}} + \mu_p r \bar{p}^2\right) - \left(G_{0\psi}^2 + G_{0\chi}^2\right)\left(\bar{\bar{p}}^2 + \mu_p r \bar{p}\cdot\bar{\bar{p}}\right)}{\left(\bar{p}^2 + \mu_p^2\right)^3} \\ &+ \int_p \frac{\left[2 G_{0\psi} G_{0\chi} \mu_p^2 - \left(G_{0\psi}^2 + G_{0\chi}^2\right)\bar{p}^2\right]\left[8 - 4\bar{p}^2 + 2r^2 \bar{p}^2 + \mu_p r (8 - \hat{p}^2)\right]}{\left(\bar{p}^2 + \mu_p^2\right)^3} \\ &- 8 \int_p \frac{\left[2 G_{0\psi} G_{0\chi} \mu_p^2 - \left(G_{0\psi}^2 + G_{0\chi}^2\right)\bar{p}^2\right]\left(\bar{\bar{p}} + \mu_p r \bar{p}\right)^2}{\left(\bar{p}^2 + \mu_p^2\right)^4} \end{aligned} \tag{57}$$

and the renormalized scalar mass squared is

$$m_{\mathrm{R}}^2 = m_0^2 + \tfrac{2}{3} g_0 \int_p \left(\hat{p}^2 + m_0^2\right)^{-1}$$

$$+ 8 \int_p \frac{2 G_{0\psi} G_{0\chi} \mu_p^2 - \left(G_{0\psi}^2 + G_{0\chi}^2\right) \bar{p}^2}{\left(\bar{p}^2 + \mu_p^2\right)^2} + m_0^2 (2\kappa Z_\phi - 1). \tag{58}$$

The wave function renormalization Z_ϕ relates the original field to the renormalized field via

$$\phi_{\mathrm{R}} = Z_\phi^{-1/2} \phi. \tag{59}$$

Correspondingly the renormalized bosonic vertex functions are defined through

$$\Gamma_{\mathrm{R}}^{(n,0)} = Z_\phi^{n/2} \Gamma^{(n,0)}. \tag{60}$$

The renormalized self-coupling g_{R} of the scalar field is defined in terms of the value of the renormalized four-point vertex function at zero momentum,

$$g_{\mathrm{R}} S_{ijkl} = -\Gamma_{\mathrm{R}}^{(4,0)}(0,0,0,0)_{ijkl}. \tag{61}$$

In one-loop perturbation theory we find

$$g_{\mathrm{R}} = g_0 - \tfrac{5}{3} g_0^2 \int_p \left(\hat{p}^2 + m_0^2\right)^{-2}$$

$$+ 48 \int_p \left(\bar{p}^2 + \mu_p^2\right)^{-4} \Big[2 G_{0\psi}^2 G_{0\chi}^2 \mu_p^4 - 4 G_{0\psi} G_{0\chi} \left(G_{0\psi}^2 + G_{0\chi}^2 + G_{0\psi} G_{0\chi}\right) \bar{p}^2 \mu_p^2$$

$$+ \left(G_{0\psi}^4 + G_{0\chi}^4\right) \left(\bar{p}^2\right)^2 \Big] + 2 g_0 (2\kappa Z_\phi - 1). \tag{62}$$

The one-loop result for the inverse fermion propagator is of the form

$$-\Gamma^{(0,2)}(p) = \begin{pmatrix} i\gamma \cdot p Z_\psi^{-1} & \mu_0 Z_\mu^{-1} \\ \mu_0 Z_\mu^{-1} & i\gamma \cdot p Z_\chi^{-1} \end{pmatrix} + \mathrm{O}(p^2), \tag{63}$$

with

$$2KZ_\mu + 1 + 2 G_{0\psi} G_{0\chi} \mu_0^{-1} \int_p \left(\hat{p}^2 + m_0^2\right)^{-1} \left(\bar{p}^2 + \mu_p^2\right)^{-1} \mu_p, \tag{64}$$

$$2KZ_\psi = 1 - G_{0\psi}^2 \int_p \left(\hat{p}^2 + m_0^2\right)^{-2} \left(\bar{p}^2 + \mu_p^2\right)^{-1} \bar{p}^2, \tag{65}$$

and $2KZ_\chi$ analogous. For the renormalized fermion fields

$$\Psi_R = Z_\Psi^{-1/2}\Psi = \begin{pmatrix} Z_\psi^{-1/2} & 0 \\ 0 & Z_\chi^{-1/2} \end{pmatrix}\Psi \tag{66}$$

the inverse propagator is

$$-\Gamma_R^{(0,2)}(p) = -Z_\Psi^{1/2}\Gamma^{(0,2)}(p)Z_\Psi^{1/2} = \begin{pmatrix} i\gamma\cdot p & \mu_R \\ \mu_R & i\gamma\cdot p \end{pmatrix} + O(p^2), \tag{67}$$

and determines the renormalized fermion mass,

$$\begin{aligned} \mu_R &= \mu_0 Z_\psi^{1/2} Z_\chi^{1/2} Z_\mu^{-1} \\ &= \mu_0 - \tfrac{1}{2}\mu_0\left(G_{0\psi}^2 + G_{0\chi}^2\right)\int_p \left(\hat{p}^2 + m_0^2\right)^{-2}\left(\bar{p}^2 + \mu_p^2\right)^{-1}\bar{p}^2 \\ &\quad - 2G_{0\psi}G_{0\chi}\int_p \left(\hat{p}^2 + m_0^2\right)^{-1}\left(\bar{p}^2 + \mu_p^2\right)^{-1}\mu_p . \end{aligned} \tag{68}$$

Finally we come to the renormalized Yukawa couplings. They are specified through the renormalized boson–fermion vertex function at zero momentum,

$$\Gamma_{R,i}^{(1,2)}(0,0,0) = Z_\phi^{1/2} Z_\Psi^{1/2}\Gamma_i^{(1,2)}(0,0,0)Z_\Psi^{1/2}, \tag{69}$$

where the index $i = 1,2$ refers to the component of ϕ_i. At one-loop order this matrix is diagonal like the bare vertex V_i but with the bare couplings $G_{0\psi}$ and $G_{0\chi}$ replaced by

$$G_{R\psi} = G_{0\psi} - G_{0\psi}^3\int_p \left(\hat{p}^2 + m_0^2\right)^{-2}\left(\bar{p}^2 + \mu_p^2\right)^{-1}\bar{p}^2 + \tfrac{1}{2}G_{0\psi}(2\kappa Z_\phi - 1), \tag{70}$$

$$G_{R\chi} = G_{0\chi} - G_{0\chi}^3\int_p \left(\hat{p}^2 + m_0^2\right)^{-2}\left(\bar{p}^2 + \mu_p^2\right)^{-1}\bar{p}^2 + \tfrac{1}{2}G_{0\chi}(2\kappa Z_\phi - 1). \tag{71}$$

The relations above form the basis for renormalized perturbation theory. They allow us to express the bare parameters of the model in terms of the renormalized ones. Every other physical, renormalized quantity, like propagators or higher vertex functions, can then be expanded perturbatively in powers of the renormalized couplings such that the coefficients depend on the renormalized masses.

On the other hand, for sufficiently small bare couplings the bare perturbative expansions themselves can be used to locate the critical points in parameter space,

i.e. those points where the renormalized masses vanish,

$$m_R = 0, \qquad \mu_R = 0. \tag{72}$$

From the perturbative expressions for m_R and μ_R one obtains the corresponding critical values for the bare masses (for $r = 1$),

$$m_{0c}^2 = -\tfrac{2}{3} g_0 \int_p (\hat{p}^2)^{-1} - 16 G_{0\psi} G_{0\chi} \int_p (\hat{p}^2/2)^2 \left[\bar{p}^2 + (\hat{p}^2/2)^2\right]^{-2}$$

$$+ 8\left(G_{0\psi}^2 + G_{0\chi}^2\right) \int_p \bar{p}^2 \left[\bar{p}^2 + (\hat{p}^2/2)^2\right]^{-2} + O\left(g_0^2, g_0 G_0^2, G_0^3\right), \tag{73}$$

$$\mu_{0c} = G_{0\psi} G_{0\chi} \int_p \left[\bar{p}^2 + (\hat{p}^2/2)^2\right]^{-1} + \ldots . \tag{74}$$

In the particular case $G_\chi = 0$, which is considered in the numerical work, we find

$$\mu_{0c} = 0, \qquad K_c = \tfrac{1}{8}, \tag{75}$$

and a quadratic equation for the critical value of κ,

$$\kappa_c^2 + \left(8 I_2 G_\psi^2 - (1 - 2\lambda)/8\right)\kappa_c - I_1 \lambda/2 = 0. \tag{76}$$

The numerical constants are

$$I_1 = \int_p (\hat{p}^2)^{-1} = 0.154933\ldots \tag{77}$$

$$I_2 = \int_p \bar{p}^2 \left[\bar{p}^2 + (\hat{p}^2/2)^2\right]^{-2} = 0.025703\ldots . \tag{78}$$

For constant λ the value of κ_c decreases with increasing G_ψ.

3.2. β-FUNCTIONS

The behaviours of the coupling constants are determined by their full β-functions. The perturbative β-functions can be calculated analytically, while the full β-functions can be studied by Monte Carlo simulations if the finite-size effects are under good control.

From the results of subsect. 3.1 the renormalization group β-functions can be derived in the one-loop approximation. The β-functions describe how the renormalized couplings change with varying cutoff if the bare couplings are held

constant. Since in our notation the inverse cutoff, namely the lattice spacing a, is set equal to one, a change of the cutoff means a simultaneous change of m_R and μ_R by the same factor. More precisely, the β-functions are defined by

$$\beta_g = m_R \frac{\partial g_R}{\partial m_R} + \mu_R \frac{\partial g_R}{\partial \mu_R}, \tag{79}$$

$$\beta_\psi = m_R \frac{\partial G_{R\psi}}{\partial m_R} + \mu_R \frac{\partial G_{R\psi}}{\partial \mu_R}, \tag{80}$$

$$\beta_\chi = m_R \frac{\partial G_{R\chi}}{\partial m_R} + \mu_R \frac{\partial G_{R\chi}}{\partial \mu_R}, \tag{81}$$

where the derivatives are to be taken at fixed bare couplings g_0, $G_{0\psi}$ and $G_{0\chi}$. Notice that all the couplings in this subsection are those in the continuum convention normalization.

The behaviours of the renormalized couplings as functions of the scale variable $\tau \equiv \log(am)^{-1}$ (where am is some mass in lattice units) in the limit $\tau \to \infty$ are governed by the infrared structure of the β-functions. We have calculated these functions in one-loop order including non-universal scaling violating terms. The resulting expressions, however, are too voluminous to be displayed here. Therefore in the following we restrict ourselves to the universal scaling parts of the β-functions, which do not depend on the masses. They can be obtained from the logarithmically divergent parts of eqs. (62), (70) and (71) and read

$$16\pi^2 \beta_g^{(1)} = \tfrac{10}{3} g_R^2 + 8N_f g_R \left(G_{R\psi}^2 + G_{R\chi}^2\right) - 48N_f \left(G_{R\psi}^4 + G_{R\chi}^4\right), \tag{82}$$

$$16\pi^2 \beta_\psi^{(1)} = 2(N_f + 1) G_{R\psi}^3 + 2N_f G_{R\psi} G_{R\chi}^2, \tag{83}$$

$$16\pi^2 \beta_\chi^{(1)} = 2(N_f + 1) G_{R\chi}^3 + 2N_f G_{R\chi} G_{R\psi}^2, \tag{84}$$

where N_f is the total number of fermion-mirror pairs and is equal to 2 in our flavour-doubled model. One can see that $g_R = G_{R\psi} = G_{R\chi} = 0$ is an infrared fixed point, therefore the continuum limit of the model is trivial unless there is some other nonperturbative nontrivial fixed point. In order to have an interacting continuum theory, one has to keep the cutoff at some finite scale higher than the typical mass scale of the theory. The renormalized couplings will depend on the cutoff scale and will go up as the cutoff is decreased. When the cutoff is as low as the mass scale, the theory ceases being an effective theory due to large effects from the scaling violation terms. Therefore, one can get upper bounds on the renormalized couplings which are cutoff dependent. We set the cutoff at several different scales and obtain the upper bounds on g_R and $G_{R\psi}$ by integrating the one-loop β-functions in the continuum from some low-energy scale, which is chosen ad hoc

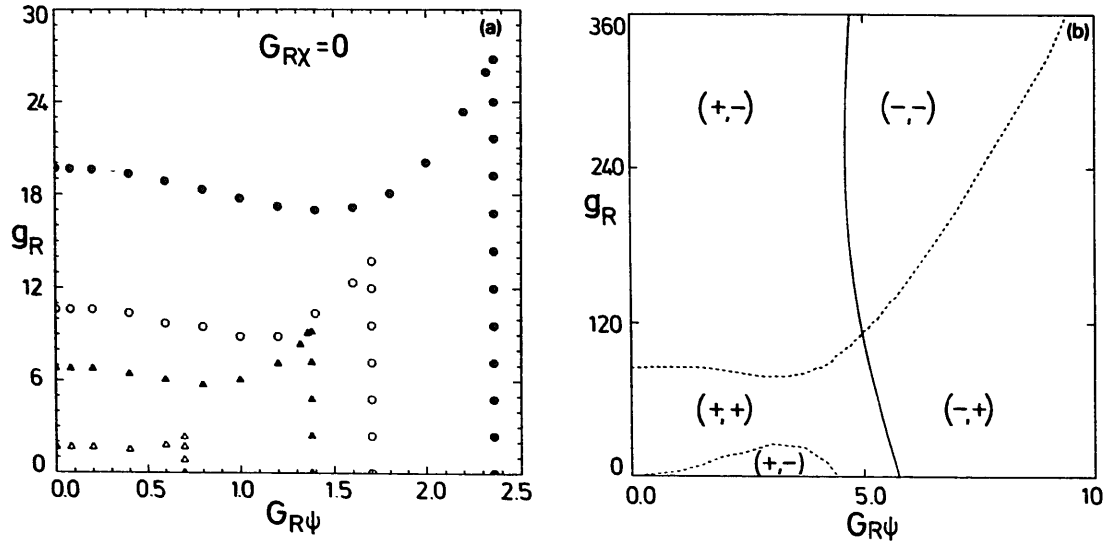

Fig. 2. (a) The joint triviality upper bounds on the renormalized scalar coupling g_R and the renormalized Yukawa coupling $G_{R\psi}$ are calculated from one-loop β-functions at $G_{R\chi} = 0$. The intrinsic cutoff is set at 1 TeV (full circles), 8 TeV (open circles), 100 TeV (full triangles) and the GUT scale (open triangles). The triviality upper limit on $G_{R\psi}$ at one-loop order is independent of the value of g_R. The limits from the vacuum stability and the Coleman–Weinberg mechanism are not shown here. (b) The zeros of the two-loop β-functions at $G_{R\chi} = 0$ are plotted. The dashed lines are zeros for β_g, while the solid line represents zeros for β_ψ.

to be 90 GeV, to the cutoff scale. We do this for the special case $G_{R\chi} = 0$. The results are shown in fig. 2a. The allowed region for g_R and $G_{R\psi}$ is smaller as the cutoff is higher, and eventually shrinks to one point at the origin indicating that the continuum limit is trivial. If the qualitative behaviours of the full β-functions are like what we see in one-loop order, then we should be able to see that in our simulations. If we plot the lines of constant physics (on which g_R, $G_{R\psi}$, $G_{R\chi}$ and $m_R/\mu_R = \text{const.}$) in the bare parameter space, then for any line along which all renormalized couplings are kept fixed at some nonzero values, the system will be driven closer to the critical line as the cutoff increases, but never really reaches the critical line. As we cross those lines and approach the criticality, we find that renormalized couplings are decreasing to zero. This is exactly what we are now exploring in the symmetric phase. Notice that in the broken phase, upper bounds on the renormalized couplings can be translated into upper bounds on the scalar and fermion masses.

It can also be easily seen that in the limit $\tau \to \infty$, among the ratios

$$x \equiv \frac{G_{R\chi}^2}{G_{R\psi}^2}, \qquad y_\psi \equiv \frac{G_{R\psi}^2}{g_R}, \qquad y_\chi \equiv \frac{G_{R\chi}^2}{g_R}, \tag{85}$$

x will stay at zero at any energy scale if $G_{0\chi}$ is set to zero, and

$$x \to 1 \tag{86}$$

otherwise. This is slightly different from what we see in the SU(2) Yukawa model where one can fix x at any arbitrary value [10, 14]. (The β-functions given in refs. [10, 14] are for $N_f = 1$.) One can also see that

$$y_\chi = 0, \qquad y_\psi \to \frac{N_f - 1 + \sqrt{N_f^2 + 38N_f + 1/2}}{24N_f}, \tag{87}$$

if $G_{0\chi} = 0$, $G_{0\psi} \neq 0$ (we always assume that $g_0 \neq 0$). If both $G_{0\chi}$ and $G_{0\psi}$ are nonzero, then we get

$$y_\psi, y_\chi \to \frac{2N_f - 1 + \sqrt{4N_f^2 + 76N_f + 1}}{48N_f} \tag{88}$$

as $\tau \to \infty$. So the one-loop equations do indicate that $G_{R\chi}$ is (approximately) zero once $G_{0\chi} = 0$.

The one-loop formulae will break down and higher-loop contributions should come in as the couplings get relatively strong. In order to estimate when the one-loop formulae become invalid, we need at least to know the two-loop β-functions.

The universal two-loop contributions can be figured out from ref. [22] in which the two-loop β-functions of a general scalar–gauge-fermion model were worked out. We rewrote the action of our model in terms of two-component left-handed fermion fields and compared the result with the standard form given in ref. [22] to read off the Yukawa coupling matrix. In this way we obtained the two-loop β-functions for our model. We write the results in the form

$$\beta_i = \beta_i^{(1)} + \beta_i^{(2)}, \tag{89}$$

with

$$(16\pi^2)^2 \beta_g^{(2)} = -\tfrac{47}{8} g_R^3 - \tfrac{40}{3} N_f g_R^2 \left(G_{R\psi}^2 + G_{R\chi}^2\right) + 8N_f g_R \left(G_{R\psi}^4 + G_{R\chi}^4\right) + 384N_f \left(G_{R\psi}^6 + G_{R\chi}^6\right), \tag{90}$$

$$(16\pi^2)^2 \beta_\psi^{(2)} = \left(\tfrac{15}{2} - 18N_f\right) G_{R\psi}^5 - 12N_f G_{R\psi}^3 G_{R\chi}^2 - 6N_f G_{R\psi} G_{R\chi}^4 - \tfrac{8}{3} g_R G_{R\psi}^3 + \tfrac{1}{9} g_R^2 G_{R\psi}, \tag{91}$$

$$(16\pi^2)^2 \beta_\chi^{(2)} = \left(\tfrac{15}{2} - 18N_f\right) G_{R\chi}^5 - 12N_f G_{R\chi}^3 G_{R\psi}^2 - 6N_f G_{R\chi} G_{R\psi}^4 - \tfrac{8}{3} g_R G_{R\chi}^3 + \tfrac{1}{9} g_R^2 G_{R\chi}. \tag{92}$$

As a double check, we also obtain the one-loop β-functions from their formulae. Their results for the one-loop contributions agree with ours.

Together with the one-loop contributions, one can roughly estimate that the one-loop β-functions become invalid when $G^2_{R\psi}, G^2_{R\chi} \sim 35$ for $N_f = 2$. One can also see that, due to the alternating signs, some new zeros of the β-functions are generated at two-loop level. It is possible that they are just the two-loop artifact because the two-loop formulae will also be invalid as the couplings become even stronger. Nevertheless, let us at the moment assume that the two-loop β-functions are qualitatively like the full ones and see what we have. As usual, we set $G_{0\chi} = 0$ for the sake of simplicity, and look at β_g and β_ψ in the (g, G_ψ)-plane. The zeros of β_g and β_ψ can be easily calculated numerically for $N_f = 2$, and are plotted in fig. 2b, where $(+, -)$, for example, denotes the region in which $\beta_\psi > 0$ and $\beta_g < 0$ etc. We actually did not calculate the zeros in the region where both couplings are very large. However, from eqs. (82)–(84) and eqs. (90)–(92), one can see that for any fixed value of g_R, the function β_g, which is equal to $\beta_g^{(1)} + \beta_g^{(2)}$ up to two-loop order, will become positive as we increase $G_{R\psi}$ indefinitely. Similarly, β_ψ will become positive as $g_R \to \infty$ for any fixed $G_{R\psi}$. Hence we believe that the lines of zeros of two-loop β-functions for very large couplings should converge to the corner at $g_R = G_{R\psi} = \infty$. The point at which the solid and dashed curves intersect each other in fig. 2b is the new fixed point up to two-loop order, and is located at $g_R \sim 120$, $G_{R\psi} \sim 5$. Suppose that the full β-functions are like this, then we should see the "effect" of this ultraviolet fixed point in our Monte Carlo data. What we should see is the following. If we measure g_R and $G_{R\psi}$ and find the lines of constant physics in the bare parameter space, those lines should converge to that new fixed point. When we approach the critical line at bare couplings greater than the fixed point values, we should encounter growing renormalized couplings as the cutoff is increasing. This qualitative picture can be easily generalized to the case where both $G_{0\psi}$ and $G_{0\chi}$ are nonzero.

3.3. FINITE-VOLUME EFFECTS

For fixed bare parameters κ, K etc. any renormalized quantity like m_R, μ_R, g_R etc. will depend on the lattice size $L^3 \times T$. We impose the renormalization conditions at $L = T = \infty$ which means that we identify

$$m_R \equiv m_R(\infty,\infty), \qquad \mu_R \equiv \mu_R(\infty,\infty), \qquad g_R \equiv g_R(\infty,\infty) \quad \text{etc.} \tag{93}$$

as the renormalized parameters. For fixed values of the bare parameters the deviation of a renormalized quantity X from its infinite-volume limit is denoted by

$$\delta X(L,T) = X(L,T) - X(\infty,\infty). \tag{94}$$

This can be calculated in renormalized perturbation theory as a power series in g_R, $G_{R\psi}$ and $G_{R\chi}$. In finite-volume perturbation theory the lattice momenta flowing in loops are restricted to the Brillouin zone (12). For momentum sums we

define the finite-volume deviations in the same way as in eq. (94),

$$\delta\int_p f(p) = \frac{1}{L^3T}\sum_p f(p) - (2\pi)^{-4}\int_0^{2\pi} \mathrm{d}^4 p f(p). \tag{95}$$

The perturbative finite volume effects to one-loop order can now be obtained directly from the results of subsect. 3.1 by replacing momentum sums by the corresponding deviations $\delta\int$ and bare parameters by renormalized ones. In the case of the fermion mass for example one obtains

$$\delta\mu_R = -\tfrac{1}{2}\mu_R\left(G_{R\psi}^2 + G_{R\chi}^2\right)\delta\int_p \left(\hat{p}^2 + m_R^2\right)^{-2}\left(\bar{p}^2 + \mu_p^2\right)^{-1}\bar{p}^2$$

$$- 2G_{R\psi}G_{R\chi}\delta\int_p \left(\hat{p}^2 + m_R^2\right)^{-1}\left(\bar{p}^2 + \mu_p^2\right)^{-1}\mu_p. \tag{96}$$

(In μ_p the bare mass μ_0 has of course also to be replaced by μ_R.) The corresponding formulae for δm_R, δg_R, $\delta G_{R\psi}$ and $\delta G_{R\chi}$ are derived in the same way and need not be displayed here. We have written a program for the numerical evaluation of these expressions which is used in the analysis of the results of the Monte Carlo simulation.

3.4. TREE UNITARITY

In this subsection, we present our calculations of the partial wave amplitudes in tree approximation, aiming at getting an independent estimate of when the renormalized Yukawa couplings are strong. These considerations are in the spirit of ref. [23].

Without loss of generality, we here consider only one pair of fermion and its mirror (i.e.: one pair of ψ and χ). We first diagonalize the fermion mass matrix by the transformation introduced in sect. 2. After the transformation, the lagrangian density of the Yukawa interactions in continuous Minkowski space-time is

$$\mathscr{L}_Y = -\bar{\psi}_{RA}\sqrt{2}\left(G_{R\alpha} - G_{R\beta}\gamma_5\right)\phi_R\psi_{RB} - \bar{\psi}_{RB}\sqrt{2}\left(G_{R\alpha} + G_{R\beta}\gamma_5\right)\phi_R^+\psi_{RA}, \tag{97}$$

where

$$G_{R\alpha} = \tfrac{1}{2}\left(G_{R\psi} + G_{R\chi}\right), \qquad G_{R\beta} = \tfrac{1}{2}\left(G_{R\psi} - G_{R\chi}\right). \tag{98}$$

Notice that we have replaced bare quantities by renormalized ones, since we will do the calculations at tree level.

We are mainly concerned with the renormalized Yukawa couplings, therefore the following two processes are considered here.

Process 1:

$$f_B(p_1) + \bar{f}_A(p_2) \to f_B(p_3) + \bar{f}_A(p_4),$$

where f and $\bar{f}$ mean fermions and anti-fermions respectively, with momenta p_i and helicities λ_i, $i = 1,\ldots,4$.

Process 2:

$$f_A(p_1) + \bar{f}_A(p_2) \to \phi(p_3) + \phi^+(p_4),$$

where the fermions f_A and $\bar{f}_A$ have helicities λ_1 and λ_2 respectively.

Now we go to the center-of-mass frame in which we have $\boldsymbol{p}_1 + \boldsymbol{p}_2 = 0$. We set

$$s = (p_1 + p_2)^2, \qquad E_1 = \tfrac{1}{2}\sqrt{s}, \qquad |\boldsymbol{p}| = \sqrt{E_1^2 - \mu_R^2}.$$

Once the z-axis is chosen to be along the direction of $\boldsymbol{p}_1$, we get

$$\boldsymbol{p}_3 = |\boldsymbol{p}|(\cos\phi \sin\theta, \sin\phi \sin\theta, \cos\theta),$$

where θ and ϕ are the azimuthal and polar angles of $\boldsymbol{p}_3$ with respect to the z-axis.

For process 1, the results for various helicity amplitudes $T_{\lambda_1\lambda_2\lambda_3\lambda_4}$ are

$$T_{++++} = \frac{8}{s - m_R^2}\left(2|\boldsymbol{p}|E_1 G_{R\alpha}G_{R\beta} - E_1^2 G_{R\beta}^2 - (E_1^2 - \mu_R^2)G_{R\alpha}^2\right),$$

$$T_{----} = \frac{-8}{s - m_R^2}\left(2|\boldsymbol{p}|E_1 G_{R\alpha}G_{R\beta} + E_1^2 G_{R\beta}^2 + (E_1^2 - \mu_R^2)G_{R\alpha}^2\right),$$

$$T_{++--} = \frac{-8}{s - m_R^2}\left(E_1^2 G_{R\beta}^2 - (E_1^2 - \mu_R^2)G_{R\alpha}^2\right),$$

$$T_{--++} = T_{++--}, \tag{99}$$

where $\lambda = +$ and $-$ denote the helicity states with left and right handedness respectively. All other amplitudes are zero.

For process 2, we get the amplitudes as

$$T_{++} = \frac{-2}{t - \mu_R^2}\left\{2\mu_R|\boldsymbol{p}|\left(\left(G_{R\beta}^2 - G_{R\alpha}^2\right) - (1 - \cos\theta)\left(G_{R\beta}^2 + G_{R\alpha}^2\right)\right)\right\},$$

$$T_{+-} = \frac{4}{t - \mu_R^2}\, e^{i\phi} \sin\theta|\boldsymbol{p}|\left(E_1\left(G_{R\alpha}^2 + G_{R\beta}^2\right) + 2|\boldsymbol{p}|G_{R\alpha}G_{R\beta}\right),$$

$$T_{-+} = \frac{4}{t - \mu_R^2}\, e^{-i\phi} \sin\theta|\boldsymbol{p}|\left(E_1\left(G_{R\alpha}^2 + G_{R\beta}^2\right) - 2|\boldsymbol{p}|G_{R\alpha}G_{R\beta}\right),$$

$$T_{--} = -T_{++}, \tag{100}$$

where $t = (p_1 - p_3)^2$.

The above amplitudes can be expanded into a partial wave series. Since

$$|\mathrm{Re}(a_J)| \leqslant \tfrac{1}{2}, \tag{101}$$

one will get upper bounds on the Yukawa couplings from various processes. The only nonzero partial wave amplitude for process 1 is $a_{J=0}$. For process 2, one can get two nonzero amplitudes: $a_{J=0}$ and $a_{J=1}$. In the relativistic limit (i.e. $s \to \infty$), we obtain the unitarity upper limits on $G_{R\psi}$ and $G_{R\chi}$ from process 1 as

$$G_{R\psi}^2 + G_{R\chi}^2 \leqslant 4\pi. \tag{102}$$

Process 2 gives us

$$G_{R\psi}^2 \leqslant 4\sqrt{2}\,\pi, \qquad G_{R\chi}^2 \leqslant 4\sqrt{2}\,\pi. \tag{103}$$

Therefore, from tree unitarity limits on the Yukawa couplings, we see that when $G_{R\psi}, G_{R\chi} \simeq 3 \sim 4$, the system is becoming strongly interacting. Notice that the upper limits from the tree unitarity are slightly more strict than the ones obtained from comparing the one-loop and two-loop terms in the β-functions.

4. Fermion hopping parameter expansion

Expansions in powers of the hopping parameters κ, K are very useful non-perturbative tools for obtaining qualitative analytic information on the behaviour of Yukawa models in the phase with unbroken symmetry. In fact, this information can also be quantitatively accurate at the edge of the scaling region (near the critical hypersurface), if high enough orders are evaluated. An example is the approximate analytic solution of O(n) symmetric ϕ^4 models by Lüscher and Weisz [24], which is based on a 14th-order scalar hopping parameter expansion. This technique turned out to be very helpful also in a study of the infinitely heavy fermion limit of our model [15]. In case of the $SU(2)_L \otimes SU(2)_R$ symmetric Yukawa model with explicit mirror fermions an 8th-order fermion hopping parameter expansion at $\kappa = 0$, $\lambda = \infty$ and $G_\psi = G_\chi$ was applied by Wagner [18]. The extension to $\lambda = 0$ and to the case of different masses within doublets has been considered in the random walk approximation in ref. [19].

In the present section the 7th-order hopping parameter expansion of the fermion propagator will be briefly discussed. More details and an extension to other quantities will be published elsewhere [25]. The bare scalar quartic coupling will be fixed to $\lambda = \infty$, but different bare Yukawa couplings will be allowed ($G_\psi \neq G_\chi$). For the hopping parameter expansion the flavour doubling is not necessary (unlike in the numerical simulation), therefore here we consider the original single flavour model (1).

As already mentioned in sect. 2, for the fermion hopping parameter expansion it is advantageous to reshuffle the left- and right-handed components of ψ and χ, in

order to obtain a diagonal kinetic term in the action. In this section we use the fermion fields ψ_A, ψ_B introduced in that section.

The basic ingredient of the hopping parameter expansion is the generating function of the single-site expectation values Z_1. Since we fix λ to infinity, the scalar field has unit length,

$$\phi_x \equiv e^{i\vartheta_x}. \tag{104}$$

The single-site action S_1 at $\kappa = K = 0$ is

$$S_1 = \bar{\psi}_A \psi_A + \bar{\psi}_B \psi_B + \bar{\psi}_A e^{i\vartheta}(G_\alpha - \gamma_5 G_\beta)\psi_B + \bar{\psi}_B e^{-i\vartheta}(G_\alpha + \gamma_5 G_\beta)\psi_A. \tag{105}$$

The logarithm of the generating function

$$Z_1(\bar{N}, N) \equiv \int [d\bar{\Psi}\, d\Psi\, d\vartheta]\, e^{-S_1 + \bar{N}\Psi + \bar{\Psi}N} \tag{106}$$

is given by the expression

$$\log Z_1(\bar{N}, N) = F(\bar{N}N) + \sum_{k=1}^{\infty} B_k \left[(\bar{N}C_1 N)^2 + (\bar{N}C_2 N)^2 \right]^k. \tag{107}$$

Here F is defined as

$$F \equiv \frac{1}{1 - G_\psi G_\chi} = \frac{1}{1 - G_\alpha^2 + G_\beta^2}, \tag{108}$$

and the numbers B_k are given by

$$B_k = \sum_{m,n=1}^{\infty} \delta_{k, n_1 + 2n_2 + 3n_3 + \ldots}\, \delta_{m, n_1 + n_2 + n_3 + \ldots} \frac{(-1)^{m-1}(m-1)!}{4^k n_1! n_2! \ldots}$$

$$\times \left(\frac{1}{1!}\right)^{2n_1} \left(\frac{1}{2!}\right)^{2n_2} \left(\frac{1}{3!}\right)^{2n_3} \ldots. \tag{109}$$

For instance, $B_1 = \frac{1}{4}$ and $B_2 = -\frac{1}{64}$. The matrices $C_{1,2}$ are

$$C_1 \equiv \begin{pmatrix} 0 & -G_\alpha + G_\beta \gamma_5 \\ -G_\alpha - G_\beta \gamma_5 & 0 \end{pmatrix}, \qquad C_2 \equiv \begin{pmatrix} 0 & -iG_\alpha + iG_\beta \gamma_5 \\ iG_\alpha + iG_\beta \gamma_5 & 0 \end{pmatrix}. \tag{110}$$

By differentiating $\log Z_1$ with respect to N and $\bar{N}$ one obtains the connected single-site expectation values $\langle \Psi_1 \bar{\Psi}_1 \Psi_2 \bar{\Psi}_2 \ldots \Psi_n \bar{\Psi}_n \rangle$.

The fermion propagator can be calculated from the single-site expectation values by summing up the hopping parameter expansion graphs on the lattice. Let

us introduce the notations

$$\chi_1(p) \equiv i \sum_{\rho=1}^{4} \gamma_\rho \frac{\partial}{\partial p_\rho} \tilde{\Delta}_\psi(p), \qquad \chi_2(p) \equiv \tilde{\Delta}_\psi(p) \xrightarrow{p\to 0} \begin{pmatrix} 0 & \chi_0 \\ \chi_0 & 0 \end{pmatrix}. \quad (111)$$

The block matrix here is in the (ψ, χ)-space. One can easily see that at zero momentum the relation to A and B introduced in eq. (14) is

$$\chi_1(p \to 0) = \tfrac{1}{2}(8 - \hat{p}^2)B, \qquad \chi_2(p \to 0) = A. \quad (112)$$

From eqs. (21) and (22) follows

$$\mu_R = \lim_{p\to 0} (8-\hat{p}^2) \frac{\chi_0}{2\sqrt{\chi_{1,\psi\psi}\chi_{1,\chi\chi}}}, \quad Z_\psi = \lim_{p\to 0} (8-\hat{p}^2) \frac{\chi_0^2}{2\chi_{1,\chi\chi}},$$

$$Z_\chi = \lim_{p\to 0} (8-\hat{p}^2) \frac{\chi_0^2}{2\chi_{1,\psi\psi}}. \quad (113)$$

The two "susceptibilities" $\chi_{1,2}$ can be expressed by the one-particle irreducible (1PI) parts $\chi_{1,2}^{(1PI)}$,

$$\chi_2 = \chi_2^{(1PI)} \left[1 - K(8-\hat{p})\chi_2^{(1PI)}\right]^{-1}$$

$$\chi_1 = \left[\chi_1^{(1PI)} + K(8-\hat{p}^2)\chi_2^{(1PI)2}\right]\left[1 - K(8-\hat{p}^2)\chi_2^{(1PI)}\right]^{-2}. \quad (114)$$

Therefore, the physical information on the fermion propagator is contained in

$$\tilde{\Delta}_\psi(p)^{(1PI)} \equiv \begin{pmatrix} 0 & F \\ F & 0 \end{pmatrix} + \sum_\mu e^{-ip_\mu} \Delta_\mu. \quad (115)$$

The expansion of Δ_μ up to 7th order in K is

$$C \equiv 16K^3F^4G_\beta^2 + 576K^5F^6G_\beta^2$$

$$+ K^7F^8\left[768G_\beta^2\left(3\left(G_\alpha^2+G_\beta^2\right)^2 + 2G_\beta^4\right) - \frac{273}{48}G_\beta^6 - 192\left(G_\alpha^2 - 15G_\beta^2\right)\right],$$

$$D \equiv 192K^7F^8\left(G_\alpha^2+G_\beta^2\right)\left[\left(G_\alpha^2+G_\beta^2\right)^2 + 16G_\beta^4\right],$$

$$\Delta_\mu = \begin{pmatrix} (C+D)(G_\alpha - G_\beta)^2\gamma_\mu & C\left(G_\alpha^2 - G_\beta^2\right) \\ C\left(G_\alpha^2 - G_\beta^2\right) & (C+D)(G_\alpha+G_\beta)^2\gamma_\mu \end{pmatrix}. \quad (116)$$

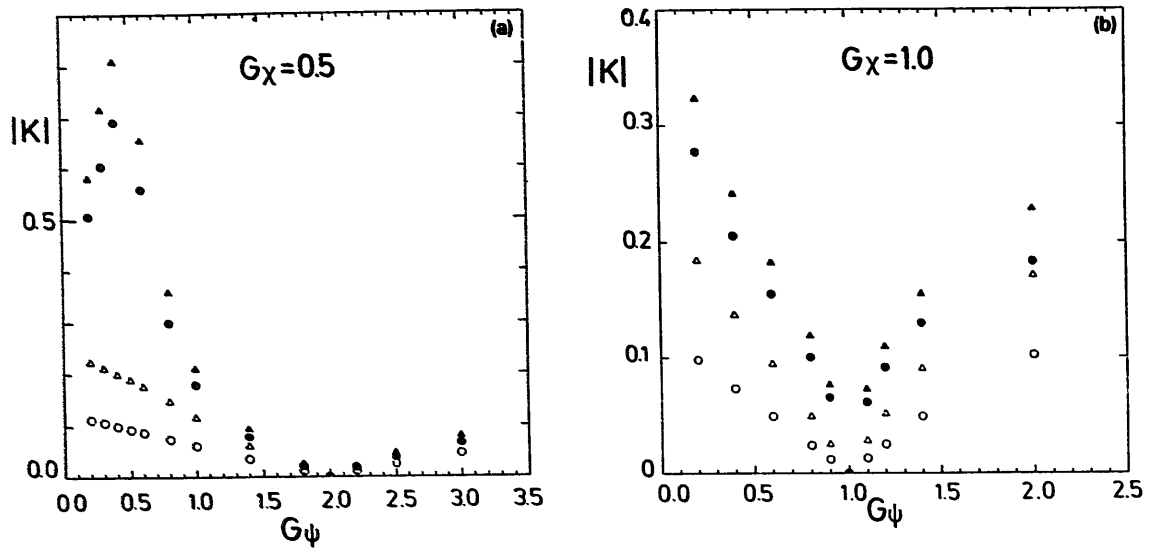

Fig. 3. (a) The critical values of K, at which the fermion mass vanishes, are calculated from a 7th-order hopping parameter expansion and are plotted at $G_\chi = 0.5$, where G_ψ and G_χ are the bare couplings in eq. (1) at $\bar{\mu} = 1$. The open circles are for the fermion mass defined at the origin of the Brillouin zone. Open triangles, full triangles and full circles are for the doublers with one, three and four π's respectively. (b) The same plot as in (a) except that $G_\chi = 1.0$ here.

An important qualitative characteristic of this series is the appearance of the powers of the product KF. Obviously, the convergence radius in K is proportional to the value of $|F|^{-1} = |1 - G_\psi G_\chi|$. Therefore, at $G_\psi G_\chi = 1$ the convergence radius of the fermion hopping parameter expansion is shrinking to zero.

Using the series in eq. (116) one can determine, up to 7th order, the critical value of the hopping parameter $K = K_{cr}$ where the fermion mass in lattice units vanishes. This can be done for every corner of the Brillouin zone (see figs. 3a, b). Only the corner giving the smallest K_{cr}-value is relevant in the continuum limit, because the masses at the other corners are still non-zero at this $K = K_{cr}$. Below $G_\psi G_\chi = 1$ the smallest K_{cr} is obtained at the 0-corner. At $G_\psi G_\chi = 1$ all the critical values shrink to zero. Above $G_\psi G_\chi = 1$ the critical values become negative, but they can be made positive by the transformation (10). If one does this, then the 4π-corner $[p = (\pi, \pi, \pi, \pi)]$ will have the smallest K_{cr}. We also note that up to this order no solution for K_{cr} was found at the 2π-corner $p = (\pi, 0, 0, \pi)$. Below $G_\psi G_\chi = 1$ no crossing of the higher branches was observed, but for larger values of $G_\psi G_\chi$ there are some crossings. For $G_\psi G_\chi \to \infty$, K_{cr} at the 0-corner is approaching K_{cr} at the 4π-corner. This suggests dynamical fermion doubling at infinite bare Yukawa couplings, in agreement with the random walk approximation [18, 19]. For $K < K_{cr}$ the renormalized mass and the wave function renormalization factor can be determined from eqs. (113)–(116). The results at the corner of the Brillouin zone which becomes critical first will be published in ref. [25].

The hopping parameter expansion shows that at zero scalar hopping parameter for infinite bare scalar self-coupling and finite bare Yukawa couplings the fermion doublers at the other corners of the Brillouin zone are probably not staying in the physical spectrum. The degeneracy of the 0-corner with the 4π-corner at ($\kappa = 0$, $\lambda = \infty$, $G_\psi G_\chi = \infty$) seems to be an exception. Of course, for other values of κ and λ the situation could be different. An interesting qualitative feature shown by the fermion hopping parameter expansion is that the critical surface for vanishing fermion mass touches the $K = 0$ surface at ($\lambda = \infty$, $G_\psi G_\chi = 1$). In this respect the singular rôle of the point ($\kappa = \kappa_{cr}$, $\lambda = \infty$, $K = 0$, $G_\psi G_\chi = 1$) found in the static fermion limit [15] is rather remarkable.

5. Numerical simulations

The Monte Carlo simulations were performed by the Hybrid Monte Carlo method [16]. As already discussed in sect. 2, this requires the flavour doubling of the fermion spectrum. The fermion degrees of freedom Ψ_x are represented by a complex pseudofermion field Φ_x. The expectation value of a purely scalar quantity $\Omega(\phi)$ is given by

$$\langle \Omega \rangle = \frac{1}{Z} \int [\mathrm{d}\phi][\mathrm{d}\phi^+][\mathrm{d}\Phi][\mathrm{d}\Phi^+] \mathrm{e}^{-S_\phi(\phi) - \Phi^+ (Q^+ Q)^{-1} \Phi} \Omega(\phi), \qquad (117)$$

where S_ϕ is the scalar part of the action (1), Q is the fermion matrix in eq. (4) and Z is the partition function

$$Z \equiv \int [\mathrm{d}\phi][\mathrm{d}\phi^+][\mathrm{d}\Phi][\mathrm{d}\Phi^+] \mathrm{e}^{-S_\phi(\phi) - \Phi^+ (Q^+ Q)^{-1} \Phi}. \qquad (118)$$

The pseudofermion field can also be used for the determination of fermionic expectation values. For instance, a general fermion bilinear expectation value in the first flavour sector (with fermion matrix Q) is obtained as

$$\langle \Psi_x \overline{\Psi}_y \rangle_1 = \frac{1}{Z} \int [\mathrm{d}\phi][\mathrm{d}\phi^+][\mathrm{d}\Phi][\mathrm{d}\Phi^+] \mathrm{e}^{-S_\phi(\phi) - \Phi^+ (Q^+ Q)^{-1} \Phi}$$

$$\times \Phi^+ (Q^+ Q)^{-1} Q^+ I_{yx} (Q^+ Q)^{-1} \Phi, \qquad (119)$$

where $(I_{yx})_{wv} = \delta_{yw} \delta_{xv}$. This can be determined during the Monte Carlo process in the same way as $\langle \Omega \rangle$.

The Monte Carlo simulations were performed on $4^3 \times 8$, $6^3 \times 12$ and $8^3 \times 16$ lattices with periodic boundary conditions in the space directions. In the (longest) time direction periodic boundary conditions were taken for the scalar field and

antiperiodic ones for the fermions. As discussed in sect. 2, this is favourable for the definition of fermionic renormalized quantities near zero four-momentum because of the smaller value of the smallest non-zero momentum in the time direction. In the molecular dynamics step typically 25 000 to 35 000 trajectories per point were calculated, with about 10% at the beginning used for equilibration. Exceptions are the two $8^3 \times 16$ points, where after 1000 equilibrating trajectories only about 2500 trajectories were measured. The number of leapfrog steps per trajectory was chosen randomly between 3 and 10. The step length was tuned so that the acceptance rate for the trajectories was near 75%. The typical average trajectory length was between 0.2 and 1.0. The necessary inversions of the fermion matrix were done by the conjugate gradient iteration, until the residuum was smaller than 10^{-8} times the length square of the input vector.

The Wilson parameter in the lattice action (1) was always chosen to be $r = 1$. As discussed before, the bare Yukawa coupling of the mirror fermion field G_χ was fixed to zero, in order to stay near the region of parameter space where in the broken phase decoupling of the mirror fermions can be expected. As it is suggested by the perturbative β-functions, and will come out as a result of the numerical calculation, $G_\chi = 0$ implies that also the corresponding renormalized coupling $G_{R\chi}$ is small. Quite generally, as we shall see, the renormalization of different quantities (like coupling or fermion doubler masses) is relatively small for $G_\psi G_\chi = 0$. The other bare Yukawa coupling G_ψ is changed between zero and O(1). For larger G_ψ our present Monte Carlo program becomes rather slow and inefficient. Therefore, we did not try higher values of G_ψ. In a forthcoming publication [9] a program written specifically for strong couplings will be used in order to explore the region with larger bare Yukawa couplings. The bare quartic scalar coupling was chosen to be $\lambda = 0.1, 1.0, 10.0$. Since the measured λ-dependence for the renormalized quantities was very small (in fact, with our statistical and systematic errors not observable), no further values of λ were considered. The remaining two bare parameters κ and K were used to tune the masses of the scalar (m_R) and fermion (μ_R). Since in the present paper we are mainly interested in the renormalization of the Yukawa couplings, we have chosen κ and K near the multicritical line in such a way that the two renormalized masses were nearly equal. Large mass ratios are disfavourable due to finite-size effects and presumably imply larger scale breaking corrections to the β-functions. With our limited computer time it was not possible to explore the finite-volume dependence of the physical quantities in a large number of points of the parameter space. Therefore, the two nearly equal masses were chosen large enough, namely $m_R \simeq \mu_R \simeq 1.0$ for $4^3 \times 8$, $m_R \simeq \mu_R \simeq 0.7$ for $6^3 \times 12$ and $m_R \simeq \mu_R \simeq 0.5$ for $8^3 \times 16$, in order that the finite-volume effects be small. The one-loop perturbative formulae for finite-volume dependence (sect. 3) show qualitatively that in these cases the finite-size effects for the observed range of couplings are less than about 5% for $G_{R\psi}$ and less than about 10% for the renormalized quartic coupling g_R. The signs of these finite-volume effects are

TABLE 1
The chosen points in the parameter space and the measured renormalized masses m_R and μ_R. Statistical errors in last numerals are in parenthesis

Label	$L^3 \times T$	λ	G_ψ	G_χ	κ	K	m_R	μ_R
A	$4^3 \times 8$	1.0	0.1	0.0	0.150	0.100	0.99(2)	1.0744(2)
B	$6^3 \times 12$	1.0	0.1	0.0	0.155	0.107	0.80(3)	0.7058(2)
C	$8^3 \times 16$	1.0	0.1	0.0	0.158	0.111	0.75(4)	0.5223(9)
D	$4^3 \times 8$	1.0	0.3	0.0	0.137	0.100	1.08(5)	1.0650(12)
E	$6^3 \times 12$	1.0	0.3	0.0	0.143	0.107	1.03(8)	0.6983(5)
F	$4^3 \times 8$	1.0	0.6	0.0	0.115	0.100	0.89(3)	1.030(2)
G	$6^3 \times 12$	1.0	0.6	0.0	0.125	0.106	0.64(4)	0.7070(14)
H	$4^3 \times 8$	1.0	1.0	0.0	0.070	0.100	0.87(6)	0.969(3)
I	$6^3 \times 12$	1.0	1.0	0.0	0.070	0.104	0.78(3)	0.749(4)
J	$8^3 \times 16$	1.0	1.0	0.0	0.060	0.108	0.50(10)	0.563(10)
K	$4^3 \times 8$	1.0	2.0	0.0	−0.090	0.093	1.05(12)	1.17(2)
L	$4^3 \times 8$	0.1	0.1	0.0	0.130	0.100	0.87(3)	1.074(3)
M	$4^3 \times 8$	0.1	0.3	0.0	0.117	0.100	1.11(5)	1.063(1)
N	$4^3 \times 8$	0.1	0.6	0.0	0.095	0.100	1.02(15)	1.016(8)
O	$4^3 \times 8$	0.1	1.0	0.0	0.040	0.100	1.07(4)	0.978(8)
P	$4^3 \times 8$	10.0	0.1	0.0	0.135	0.100	0.86(4)	1.0736(4)
Q	$4^3 \times 8$	10.0	0.3	0.0	0.117	0.100	1.05(9)	1.061(2)
R	$4^3 \times 8$	10.0	0.6	0.0	0.100	0.100	0.82(14)	0.996(8)
S	$4^3 \times 8$	10.0	1.0	0.0	0.030	0.100	1.1(1)	0.99(2)

TABLE 2
Some global expectation values in the points with label defined in table 1. l is defined in eq. (120), $|\phi|$ denotes the absolute value of the average scalar field. The other notations are self-explanatory. Statistical errors in last numerals are given in parenthesis

	l	$\langle \chi_x \bar{\psi}_x \rangle$	$\langle \psi_{Lx} \phi_x^+ \bar{\psi}_{Rx} \rangle$	$\langle \chi_{Lx} \phi_x \bar{\chi}_{Rx} \rangle$	$\langle \lvert\phi\rvert \rangle$	$\langle \lvert\phi_x\rvert \rangle$
A	0.1661(4)	3.9712(3)	0.0026(2)	−0.1676(1)	0.098(1)	0.8600(1)
B	0.1694(5)	3.9105(2)	0.0035(2)	−0.1629(1)	0.050(3)	0.8619(2)
C	0.1735(4)	3.8844(3)	0.0042(2)	−0.1610(2)	0.030(3)	0.8628(2)
D	0.1532(4)	3.9663(3)	0.0072(2)	−0.4968(4)	0.086(4)	0.8556(5)
E	0.1587(9)	3.9044(3)	0.0097(1)	−0.4829(4)	0.041(3)	0.8576(4)
F	0.1422(4)	3.9526(5)	0.0136(2)	−0.9809(4)	0.0867(7)	0.85299(12)
G	0.1634(4)	3.8869(3)	0.0195(2)	−0.9632(2)	0.058(2)	0.85915(12)
H	0.1291(3)	3.9253(5)	0.0195(2)	−1.6038(6)	0.0858(14)	0.8492(2)
I	0.1412(4)	3.8619(3)	0.0257(1)	−1.5664(3)	0.0497(17)	0.85266(11)
J	0.1402(16)	3.8305(10)	0.0285(4)	−1.5411(6)	0.045(8)	0.8523(3)
K	0.076(2)	3.891(2)	0.019(1)	−3.086(3)	0.070(6)	0.8393(5)
L	0.1911(11)	3.9712(5)	0.0034(3)	−0.2015(3)	0.120(3)	0.9048(5)
M	0.165(2)	3.9654(6)	0.0086(3)	−0.586(1)	0.092(4)	0.893(1)
N	0.159(3)	3.9488(8)	0.0163(5)	−1.153(5)	0.102(15)	0.889(2)
O	0.1182(10)	3.929(2)	0.0191(4)	−1.828(2)	0.077(3)	0.8720(5)
P	0.1586(12)	3.9710(4)	0.0034(3)	−0.1917(3)	0.117(5)	0.97199(5)
Q	0.135(2)	3.9661(5)	0.0081(3)	−0.5717(3)	0.092(7)	0.97088(8)
R	0.144(4)	3.946(2)	0.0178(7)	−1.1383(7)	0.12(2)	0.9712(2)
S	0.090(2)	3.930(2)	0.0177(5)	−1.871(1)	0.095(8)	0.9693(2)

opposite: positive for $G_{R\psi}$ and negative (as in the pure ϕ^4-model [12]) for g_R. The estimated finite-volume effects for the masses are below 10% for m_R and only a few percent for μ_R (both masses are expected to be larger in a finite volume than in the infinite-volume limit). Since the inverse masses are scaled roughly by the linear extension of the volume, the change of the finite-volume effects between different lattices can be expected even smaller. The time extension $T = 2L$ of the lattices is large enough for the good determination of the masses. Especially, the smallest fermion momentum allows the extraction of the fermion mass with an error which is probably less than 10%. For instance, a test run at vanishing coupling on $4^3 \times 8$ lattice and $K = 0.1$ gave a fermion mass $\mu_R = 1.076$, instead of the correct $L = T = \infty$ value $\mu_R = 1.000$. The scalar mass m_R was determined by a cosh fit of the time slice correlations of the scalar field at time distances $\geqslant 1$.

The tuning of the masses was done in shorter runs. As a first orientation for the position of the multicritical line we took the one-loop perturbative formula (see sect. 3). The tuning was unproblematic for smaller G_ψ, but near $G_\psi = 1$ life was harder due to the slower equilibration. The points chosen for large statistics runs are summarized in table 1. Some global expectation values in these points are collected in table 2. The results for the zero momentum renormalized couplings and for the wave function renormalization factors, as defined in sect. 2, are included in table 3. The renormalized quartic coupling could not be determined

TABLE 3
Renormalized couplings and Z-factors in the points with label defined in table 1. Statistical errors in last numerals are given in parenthesis

	$G_{R\psi}$	$G_{R\chi}$	Z_ϕ	Z_ψ	Z_χ
A	1.10(2)	−0.13(3)	3.04(3)	4.446(11)	4.418(9)
B	0.84(9)	−0.28(6)	2.77(16)	4.12(3)	4.11(3)
C	1.1(3)	0.1(3)	2.5(3)	3.96(8)	3.90(7)
D	3.11(9)	−0.39(4)	2.79(14)	4.345(18)	4.436(17)
E	2.7(2)	−0.56(6)	2.8(4)	4.01(2)	4.10(3)
F	4.7(2)	−0.75(14)	1.93(3)	4.05(2)	4.35(2)
G	4.8(2)	−0.7(1)	2.26(9)	3.70(2)	4.13(2)
H	6.7(4)	−1.0(2)	1.69(4)	3.48(3)	4.36(2)
I	7.66(16)	−1.06(7)	2.50(9)	3.41(3)	4.28(2)
J	7.2(6)	−0.9(3)	3.0(4)	3.08(11)	4.15(5)
K	12.6(1.2)	−1.0(5)	2.0(3)	3.21(12)	4.81(11)
L	1.23(6)	−0.09(5)	3.54(6)	4.44(2)	4.44(2)
M	3.37(12)	−0.38(9)	3.3(2)	4.31(2)	4.43(2)
N	6.1(5)	−0.89(11)	3.4(3)	3.90(7)	4.38(2)
O	7.5(4)	−1.2(2)	2.24(12)	3.53(6)	4.41(4)
P	1.16(4)	−0.11(4)	3.24(10)	4.44(2)	4.42(2)
Q	3.53(13)	−0.50(6)	3.0(3)	4.31(3)	4.43(2)
R	5.5(4)	−0.82(6)	2.8(3)	3.76(4)	4.33(3)
S	7.9(7)	−1.7(3)	3.1(5)	3.60(13)	4.40(3)

with our statistics (the statistical errors were typically about 100%), therefore it is not included in the table. (For the estimates of finite-size effects we arbitrarily took $g_R = 40$, a large value roughly equal to the tree level unitarity limit.)

As it can be seen in table 1, the values of the fermion hopping parameter K for the given masses are not changing much with the bare couplings λ, G_ψ. At the same time, the values of the scalar hopping parameter κ are strongly decreasing as a function of G_ψ. Eventually, the point "K" at $G_\psi = 2.0$ is already at negative κ. This implies that the multicritical line, where both masses vanish, is going to negative values for large G_ψ. This seems to be a general feature in all Yukawa models investigated up to now (see e.g. refs. [2–8]). The normalized link expectation value

$$l \equiv \frac{\langle \phi^+_{x+\hat{\mu}} \phi_x \rangle}{\langle |\phi_x| \rangle^2} \tag{120}$$

shown in table 2 is also decreasing for increasing G_ψ. This could be a hint for the appearance of anti-ferromagnetic phases at large G_ψ and large negative κ [2–8].

An important question for the non-perturbative investigations of lattice Yukawa models is, whether the fermion species doublers at different corners of the Brillouin zone are heavy enough to be decoupled from the physical spectrum. The answer is clearly yes in the points of bare parameter space (with $G_\chi = 0$), which we investigated up to now. A typical example is shown in fig. 4 at $\lambda = 1$ on $6^3 \times 12$ lattices. The large mass of the fermion doublers is in accordance with lattice perturbation theory and fermion hopping parameter expansion (see sects. 3 and 4). Comparing the results on different lattices one can see that for decreasing physical mass at the 0-corner the masses at the other corners decrease by about the same amount. Therefore, the ratio of doubler masses to the physical mass becomes larger.

As it can be seen from table 3 and figs. 5a, b, the renormalized Yukawa coupling $G_{R\psi}$ is rising approximately linearly with G_ψ. The values at $G_\psi \leqslant 0.3$ are, within errors, equal to the unrenormalized coupling $G_{0\psi}$ in eq. (46). However, at $G_\psi = 1.0$, where κ starts to strongly decrease, $G_{R\psi}$ is substantially smaller than $G_{0\psi}$. The value of $G_{R\psi}$ at $G_\psi = 1.0$ is about twice the tree unitarity limit in eq. (102). According to the point "K" at $G_\psi = 2.0$ the increase of $G_{R\psi}$ is still continuing. Nevertheless, this point has less statistics and is not very well tuned because of the inefficiency of the present program at large G_ψ.

There seems to be no strong dependence of the renormalized Yukawa coupling $G_{R\psi}$ on the renormalized masses. Since the coupling is rather strong at $G_\psi = 1.0$, the change according to the one-loop perturbative β-function (which should be valid near the multicritical line for fixed bare couplings and fixed ratio of the renormalized masses) would be much larger. For instance, at ($G_{R\psi} = 7.0$, $G_{R\chi} =$

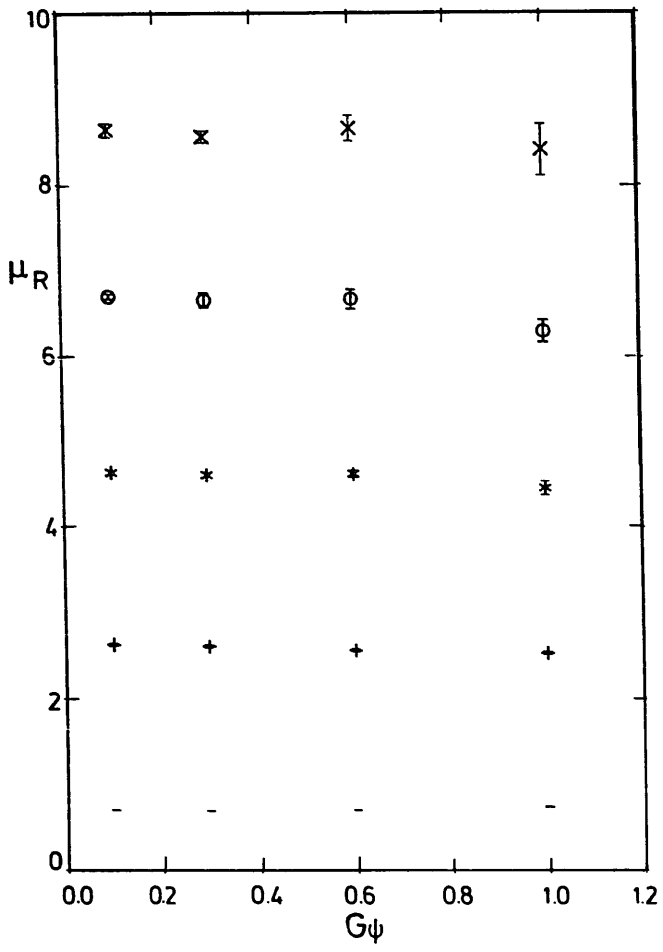

Fig. 4. The fermion masses at the different corners of the Brillouin zone on $6^3 \times 12$ lattice at $\lambda = 1.0$ as a function of the bare Yukawa coupling G_ψ. The masses increase monotonously with the increasing number of π-values in the lattice momentum.

0.0) and a logarithmic scale change $\Delta\tau = \log 2$, the one-loop β-function in eq. (83) gives $-\beta_\psi \Delta\tau \simeq -9$. Such a change is definitely excluded by our numerical data. The renormalized Yukawa coupling stays constant within errors for increasing cutoff and certainly does not decrease by such an amount. Of course, there is no reason why the one-loop β-function should be correct in a point where the absolute values of the two-loop terms are already larger than the one-loop contribution.

The renormalized Yukawa coupling of the mirror fermion field $G_{R\chi}$ is substantially smaller than $G_{R\psi}$, in agreement with our expectations. The dependence of the renormalized quantities on the bare quartic coupling λ is small, in fact not observable with our errors (see fig. 5b). Since, the average length of the scalar field is very close to 1 already at $\lambda = 10.0$ (according to table 2 it is about 0.97), no substantial change can be expected between $\lambda = 10.0$ and $\lambda = \infty$. Therefore, apart from a few test runs, we did not perform longer numerical simulations for $\lambda = \infty$.

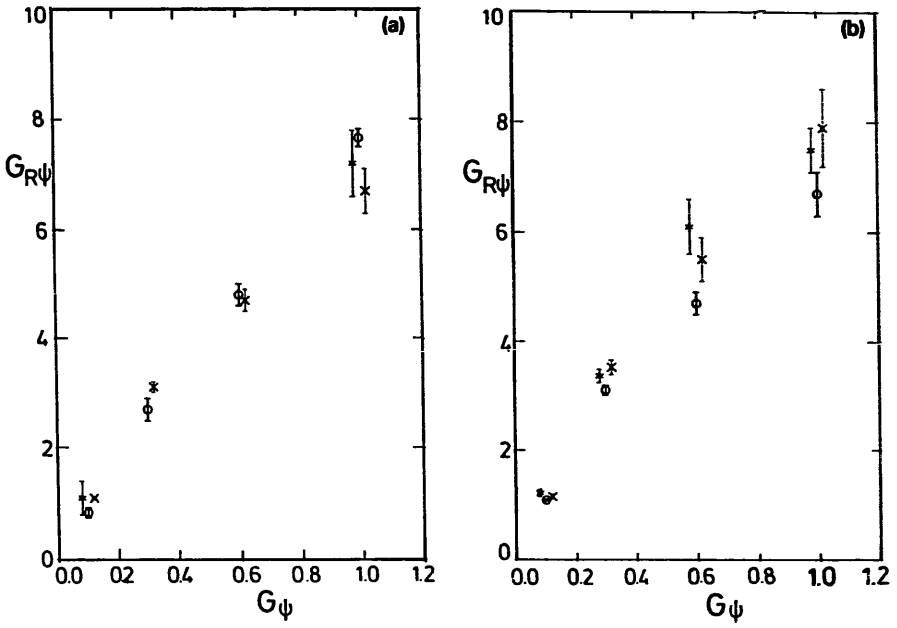

Fig. 5. (a) The renormalized Yukawa coupling $G_{R\psi}$ as a function of the bare coupling G_ψ at $\lambda = 1.0$ on $4^3 \times 8$ lattice (crosses), $6^3 \times 12$ lattice (circles) and $8^3 \times 16$ lattice (stars). The points at a given value of G_ψ are horizontally shifted a little in order to display better the error bars. (b) The same as (a) on $4^3 \times 8$ lattice for different values of the bare quartic coupling: at ($\lambda = 0.1$; stars), ($\lambda = 1.0$; circles) and ($\lambda = 10.0$; crosses).

Since the λ-dependence seems to be very weak, in the future one can concentrate the simulations (at least for $G_\chi = 0$) to a single, large λ.

6. Discussion and summary

The cutoff dependent upper limit on the renormalized quartic- and Yukawa-couplings near the infrared stable gaussian fixed point in chiral Yukawa models is an important issue for the understanding of the Higgs–Yukawa sector of the Standard Model. In the present paper the behaviour of the renormalized Yukawa couplings was investigated in the symmetric phase of a $U(1)_L \otimes U(1)_R$ symmetric lattice Yukawa model with explicit mirror fermions. We started at small bare couplings ($\lambda = 0.1$, $G_\psi = 0.1$) in the perturbative region near the gaussian fixed point and then increased the couplings up to ($\lambda = 10.0$, $G_\psi = 1.0$). The bare Yukawa coupling of the mirror fermion field was fixed to $G_\chi = 0$, in order to stay near the region of parameter space where in the broken phase decoupling of the mirror fermions can be expected. In the numerical simulations practically no dependence of the renormalized Yukawa coupling $G_{R\psi}$ on the bare quartic coupling λ was observed. $G_{R\psi}$ rises approximately linearly in the whole range as a function of the bare Yukawa coupling G_ψ. This rise is presumably continued

beyond $G_\psi = 1$, as it is suggested by a (numerically difficult) simulation at $G_\psi = 2.0$. The obtained values of the renormalized Yukawa coupling $G_{R\psi}$ at $G_\psi = 1.0$ are about twice the tree unitarity limit. Within out statistical and systematical errors of the order of 10%, no dependence on the masses in lattice units between $m_R \simeq \mu_R \simeq 1.0$ and $m_R \simeq \mu_R \simeq 0.5$ was observed.

Taken at face value, the results of the numerical simulation imply that the upper limit on the renormalized Yukawa coupling, at a cutoff corresponding to masses in lattice units of about 0.5, is at least 2 or 3 times larger than the tree unitarity limit. This is different from pure ϕ^4-models, where the corresponding upper limit is roughly equal to the tree unitarity limit (for references see ref. [1], and in particular for the symmetric phase [12, 26]). Since the change of the renormalized Yukawa coupling between masses of about 1.0 and 0.5 in lattice units is small, the β-function describing this change is small, much smaller than the one-loop β-function. The qualitative behavior is closer to the two-loop β-function which implies a non-trivial ultraviolet stable fixed point at large couplings, but the couplings are so large that neither the one-loop nor the two-loop approximation is reliable. Still one has to keep in mind that the large values of the measured renormalized Yukawa coupling can be caused by some non-perturbative non-trivial critical structure at large couplings.

The observed behaviour of the renormalized Yukawa coupling as a function of the bare Yukawa coupling does not necessarily contradict the previous numerical studies of simple Yukawa models. The effect of the virtual fermion loops on renormalized Yukawa couplings may be large, therefore it is difficult to compare with quenched calculations. The unquenched study of the Yukawa model with a real scalar field and staggered fermions [27] was restricted to a rather limited range of bare Yukawa couplings (in the statistical physical parametrization) near the perturbative region. In the corresponding range one obtains quite similar results in our model, too. (Note, however, that the value of the bare Yukawa coupling cannot easily be transferred from one model to another. Comparing the values of renormalized couplings one obtains that the range in [27] is similar to $G_\psi \simeq 0.15$ in our case.) This is one place where the advantage of studying the behaviour of renormalized Yukawa couplings in the symmetric phase becomes manifest, because we can much more easily control finite-volume effects in a wide range of bare Yukawa couplings.

A possibility to make the physical situation in this Yukawa model more similar to the pure ϕ^4-model would be that the scaling region, which in the ϕ^4-model starts near masses of about 0.5 in lattice units, could begin here only at much smaller masses. In this case the present results could be influenced by large lattice artifacts. The large renormalized Yukawa coupling could gradually decrease to smaller values before the scaling region at much smaller masses is reached. Numerical simulations with high statistics on larger lattices are required for the investigation of this question.

The Monte Carlo calculations for this paper have been performed on the CRAY Y-MP of HLRZ, Jülich.

References

[1] J. Jersák, HLRZ Jülich preprint 89-45 (1989), *in* Proc. 8th INFN Eloisatron Project Workshop, Erice, 1989, to be published
[2] A.M. Thornton, Phys. Lett. B227 (1989) 434
[3] Y. Shen, J. Kuti, L. Lin and P. Rossi, Nucl. Phys. B (Proc. Suppl.) 9 (1989) 99
[4] S. Aoki, I-H. Lee, D. Mustaki, J. Shigemitsu and R. E. Shrock, Stony Brook preprint ITP-SB-89-93 (1990);
S. Aoki, I-H. Lee, J. Shigemitsu and R. E. Shrock, Phys. Lett. B243 (1990) 403
[5] J. Berlin, A. Hasenfratz, U.M. Heller and M. Klomfass, FSU-SCRI preprint 90-15 (1990)
[6] W. Bock, A.K. De, K. Jansen, J. Jersák, T. Neuhaus and J. Smith, Jülich HLRZ preprint 90-14 (1990);
W. Bock and A.K. De, Phys. Lett. B245 (1990) 207
[7] M.A. Stefanov and M.M. Tsypin. Phys. Lett. B236 (1990) 344
[8] J. Smit. Nucl. Phys. B (Proc. Suppl.) 17 (1990) 3
[9] L. Lin, J.P. Ma, I.Montvay, G. Münster and H. Wittig, in preparation
[10] I. Montvay, Phys. Lett. B199 (1987) 89
[11] A. Borrelli, L. Maiani, G.C. Rossi, R. Sisto and M. Testa, Phys. Lett. B221 (1989) 360
[12] I. Montvay and P. Weisz, Nucl. Phys. B290 [FS20] (1987) 327;
I. Montvay, G. Münster and U. Wolff, Nucl. Phys. B305 [FS23] (1988) 143;
C. Frick, K. Jansen, J. Jersák, I. Montvay, G. Münster and P. Seuferling, Nucl. Phys. B331 (1990) 515
[13] A. Borrelli, L. Maiani, G.C. Rossi, R. Sisto and M. Testa, Nucl. Phys. B333 (1990) 335
[14] I. Montvay, Nucl. Phys. B (Proc. Suppl.) 4 (1988) 443
[15] L. Lin, J.P. Ma and I. Montvay, Z. Phys. C48 (1990) 355
[16] S. Duane, A.D. Kennedy, B.J. Pendleton and D. Roweth, Phys. Lett. B195 (1987) 216
[17] H.B. Nielsen and M. Ninomiya, Nucl. Phys. B185 (1981) 20; [Erratum: B195 (1982) 541]
[18] C.E.M. Wagner, Ph.D. Thesis, University of Hamburg (1989); DESY preprint 89-083
[19] K. Farakos, G. Koutsoumbas and I. Montvay, Z. Phys. C47 (1990) 641
[20] I. Montvay, Nucl. Phys. B307 (1988) 389
[21] K.G. Wilson, *in* New phenomena in subnuclear physics, Part A, Erice, 1975, ed. A. Zichichi (Plenum, New York) p. 69
[22] M.T. Vaughn, Z. Phys. C 13 (1982) 139;
M.E. Machacek and M.T. Vaughn, Nucl. Phys. B236 (1984) 221; B249 (1985) 70
[23] M. Chanowitz, M. Furman and I. Hinchliffe, Nucl. Phys. B153 (1979) 402
[24] M. Lüscher and P. Weisz, Nucl. Phys. B290 [FS20] (1987) 25; B295 [FS21] (1988) 65; B318 (1989) 705
[25] K. Farakos and G. Koutsoumbas, in preparation
[26] J. Kuti, L. Lin and Y. Shen, *in* Lattice Higgs Workshop, ed. B. Berg et al. (World Scientific, Singapore. 1988) p. 140
[27] I-H. Lee, J. Shigemitsu and R.E. Shrock, Nucl. Phys. B330 (1990) 225